AN ABSTRACT OF THE THESIS OF

Victor Joseph Rosato (Name) for the Master of Science (Degree)

in Oceanography (Major) presented on 28 December 1973 (Date)

Title: PERUVIAN DEEP-SEA SEDIMENTS: EVIDENCE FOR CONTINENTAL ACCRETION

Abstract approved: Redacted for privacy

L. D. Kulm

In order to determine whether the sediments found on the landward wall of the Peru Trench are accreted Nazca Plate sediments, the clay mineralogy and organic carbon contents of 52 surface samples were submitted to factor analysis. Q-mode factor analysis resolved the data from the Nazca Plate and Peru continental margin into three factors. The most important factor (oceanic assemblage) is strongly associated with Nazca Plate sediments and is comprised of smectite and aeolian illite. In contrast, upper continental margin sediments are dominated by either of the two continental factors (A or B). The principal difference between the continental factors is that mixed-layer smectite-chlorite clays are characteristic only of continental assemblage A. Lower continental margin sediments are characterized by either an oceanic or continental factor dominance.

The boundary between sediments dominated by the oceanic

factor and those dominated by the continental factor was as much as 100 km to the west of its present position earlier in the Quaternary. The seaward shift in the boundary is attributed to westward shoreline displacement in response to glacially-induced sea level changes, increased erosion rates on land during more humid times, and deposition of continental factor dominated sediments seaward of the present Peru Trench axis.

Quaternary sediments from 27 cores reveal minor fluctuations with time in factor loadings in Nazca Plate and upper continental margin cores and significant variations in some areas near the trench axis and on the middle to lower continental slope. Displacement of oceanic sediments into areas with continental sediments is determined with respect to the factor dominance boundary. Using this method, continental accretion is indicated for five cores, located up to 3000 m above the trench floor. One core on the middle continental slope off Lima, Peru, contains diatom-rich Quaternary dolomite that probably originated as calcareous sediment on the Nazca Ridge. If this is true, left-lateral strike-slip motion of the Nazca Ridge along the Peru Trench axis is indicated.

The bulk of the 28 cores recovered from the acoustically complex landward wall of the Peru Trench contain sand-silt turbidites of continental origin. Even though there is a distinct overprint of terrigenous sedimentation, accreted oceanic sediments can be

recovered in a tectonically active convergent plate boundary.

Peruvian Deep-Sea Sediments: Evidence for Continental Accretion

by

Victor Joseph Rosato

A THESIS

submitted to

Oregon State University

in partial fulfillment of
the requirements for the
degree of

Master of Science

June 1974

APPROVED:

Redacted for privacy

Associate Professor in Oceanography
in charge of major

Redacted for privacy

Dean of the School of Oceanography

Redacted for privacy

Dean of Graduate School

Date thesis is presented 28 December 1973

Typed by Marjorie Wolski for Victor Joseph Rosato

ACKNOWLEDGEMENTS

I have many people to thank for helping me in various ways during the preparation of this thesis. Foremost among them is Dr. LaVerne D. Kulm. Without his suggestions and encouragement, this work would not have been done. Special thanks are due Drs. G. Ross Heath, Ted C. Moore, Johanna M. Resig, and Moyle E. Harward for many informative discussions. I thank Drs. Arthur Boucot and Steve Johnson for serving on my committee, and Dr. Heath for reviewing an earlier draft of the thesis. Roger Prince and Chiye Yamashiro made many constructive comments. Nick Pisias provided invaluable help with the computer analysis.

The assistance of Harriet Lorz, Chris Moser and Carla Rathbun in the laboratory was appreciated.

Dr. S. B. Weed of North Carolina State College supplied unpublished information on the clay mineralogy of Peruvian soils. Roy Capo made available the samples from Lamont-Doherty Geological Observatory, which were from cores collected under ONR grant N00014-67-A-0108-0004 and NSF grant GA-35454. This research was funded by NSF grant GX-28675 under the IDOE Nazca Plate Project.

TABLE OF CONTENTS

TABLE OF CONTENTS, Continued:

LIST OF FIGURES

LIST OF FIGURES, Continued

LIST OF TABLE

PERUVIAN DEEP-SEA SEDIMENTS: EVIDENCE FOR CONTINENTAL ACCRETION

INTRODUCTION

Studies of Pacific trenches in the last few years have revealed basic similarities in their shallow structure. In the Manila Trench, Japan Trench (Ludwig and others, 1966, 1967), Middle America Trench (Ross and Shor, 1965), Aleutian Trench (von Huene and Shor, 1969; von Huene, 1972) and the Peru-Chile Trench (Scholl and others, 1968, 1970; Kulm and others, 1973) an acoustic basement (probably layer 2) dips gradually toward land in a series of normal faults that offset the overlying sediments. In the trenches pelagic sediments are believed to be unconformably overlain by more reflective, horizontal to gently tilted turbidites. The landward wall of the trenches is commonly steep and often appears as an area of superimposed hyperbolic or incoherent reflectors on seismic reflection records.

Various models have been proposed for tectonic processes at these convergent plate boundaries. In most of the models, the fate of pelagic sediments and the composition of the landward wall of the trench are uncertain. In Malahoff's (1970) model a gravity fault occurs at the trench surface which becomes a thrust fault at depths of 30 to 40 km beneath the continent. In this case pelagic sediments would be underthrust beneath the continent. In Seyfert's (1969)

model, pelagic sediments and turbidites deposited in the trench are folded, faulted, and thickened at the base of the continental slope before they are subducted. Oxburgh and Turcotte (1971) proposed two models for convergent plate boundaries. In their overthrust model, part of the oceanic sedimentary layer decouples from the descending plate and is driven up as a thrust sheet covering the trench wall. The front of the arc grows by the successive stacking up of imbricate slices. In the underthrust model, sedimentary material is dragged down the Benioff Zone and added to the underside of the continental crust. Seely and others (1974) have shown seismic profiles from the Middle America Trench that suggest that imbricate thrusts stack up beneath the foot of the continental slope, with each successive thrust uplifting the older material. As the continental slope becomes oversteepened, faulting and slumping may occur, exposing older accreted sediments.

The principal problem with these models is understanding how a compressive (convergent) boundary produces normal faulting on the seaward side of the trench, undeformed trench fill, and an acoustically complex landward wall of the trench. A problem in testing the models is the poor resolution of single channel reflection systems and the lack of drill hole data.

The Deep Sea Drilling Project has had some success in resolving the acoustic basement on the landward walls of trenchs. On

DSDP Leg 31, structures associated with subduction and accretion in the Nankai Trough were pierced by Hole 298. Sediments recovered on the lowermost slope were consolidated Pleistocene trench sediments that had developed a distinct cleavage (Ingle and others, 1973). Results of DSDP Leg 18 suggest that Cascadia Basin sediments are being folded and uplifted onto the Oregon continental margin at Site 175 (von Huene and Kulm, 1973). Site 181, on the lower continental slope off Alaska, recovered an upper hemipelagic and turbidite sequence and a lower unit consisting of deformed and compacted mud and silt. The provenance of the lower unit is uncertain because its general lithology is similar to that of the abyssal plain, trench, and lower continental slope.

Oregon State University (OSU) and the Hawaii Institute of Geophysics (HIG) Nazca Plate studies off Peru during 1971 and 1972 suggest that the acoustic basement at the foot of the continental slope might be any one of the following: (1) compacted, deformed deep-sea pelagic sediments, (2) coarse-grained turbidites or material slumped from the upper continental margin, (3) hemipelagic sediments, or (4) exposures of older sedimentary, igneous or metamorphic rocks. Within the area investigated in this thesis, which lies between 72° and 88°W and 5° and 18°S (Figure 1), the hyperbolic diffractions on seismic reflection profiles across the base of the continental slope could also indicate fault scarps or folds.

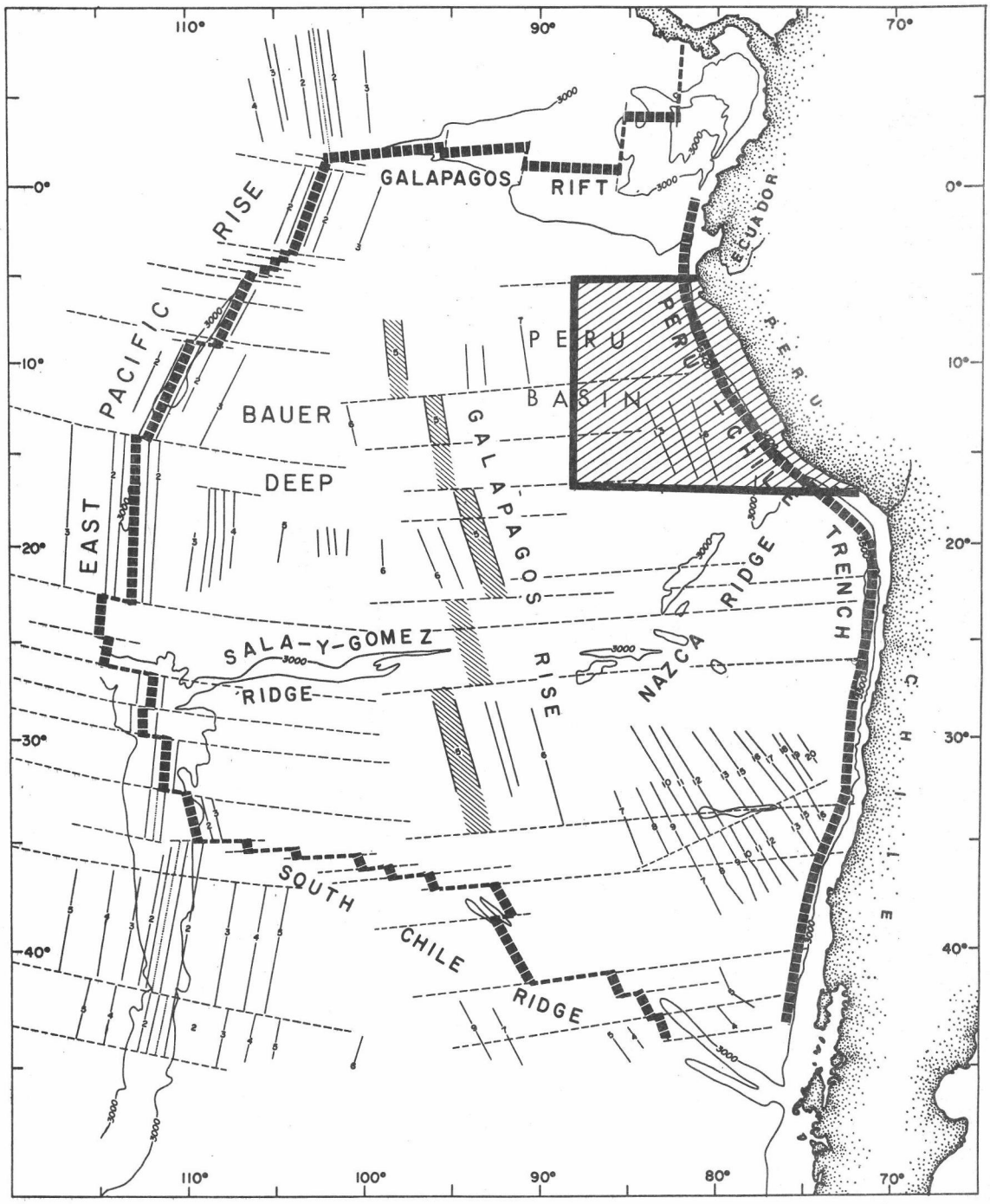

Figure 1. Nazca Plate and adjacent South America continent. The area studied is hatchured. Magnetic anomalies, ridge crests and fracture zones after Herron (1972).

If the acoustic basement on the lower continental slope off Peru is composed of accreted pelagic sediments, it should be apparent in piston cores collected in this region. There are distinct differences in lithology between continental margin and Nazca Plate sediments (Rosato and others, 1973). Since deposition rates are fairly low compared to other continental margins (10-30 cm/1000 yr; Lisitzin, 1972), older sediments may be exposed. Turbidites are restricted to the trench and continental margin except for recently discovered uplifted basins on the seaward side of the Peru Trench (Prince, 1974). Since fine-grained sediments are found on both sides of the trench, it is necessary to use such parameters as clay mineralogy and organic carbon content to indicate provenance.

The main objectives of this study are to (1) characterize the sediments on the Peruvian continental margin and the northeastern Nazca Plate, and (2) determine whether the sediments found on the acoustically complex landward wall of the Peru Trench are continental, or deep-sea sediments that have been scraped off the descending oceanic plate.

METHODOLOGY

Sampling

Appendix I contains a complete list of all the samples analyzed.

Figure 2 gives the generalized bathymetry and the locations of the cores described. Piston cores, free-fall cores and multiple gravity cores were collected by OSU and HIG. Core locations were determined by satellite navigation and bathymetry. Additional sediment samples were provided by Lamont-Doherty Geological Observatory. Most surface samples came from the uppermost undisturbed section of trigger weight cores.

Seismic Reflection Profiles

Seismic reflection profiles (OSU) were made using 40 in^3 air guns as the source and a Teledyne hydrophone streamer coupled to a Huckaby amplifier as the receiver. Filter frequencies were generally between 30-160 Hz. HIG used a 300 in^3 air gun as a seismic source, a standard single channel recording system, and filter frequencies set at 40-100 Hz.

Clay Mineral Preparation

Clay mineral preparation consisted of various chemical pretreatments to remove carbonates (acetic acid buffered to pH 5), amorphous Fe-Mn hydroxyoxides (Na-citrate, dithionite method of Mehra and Jackson, 1960), and opal (0.2 M Na_2CO_3). All samples were treated in the same manner. Following Mg-saturation and Stokesian settling, three oriented, silver-backed X-ray slides were

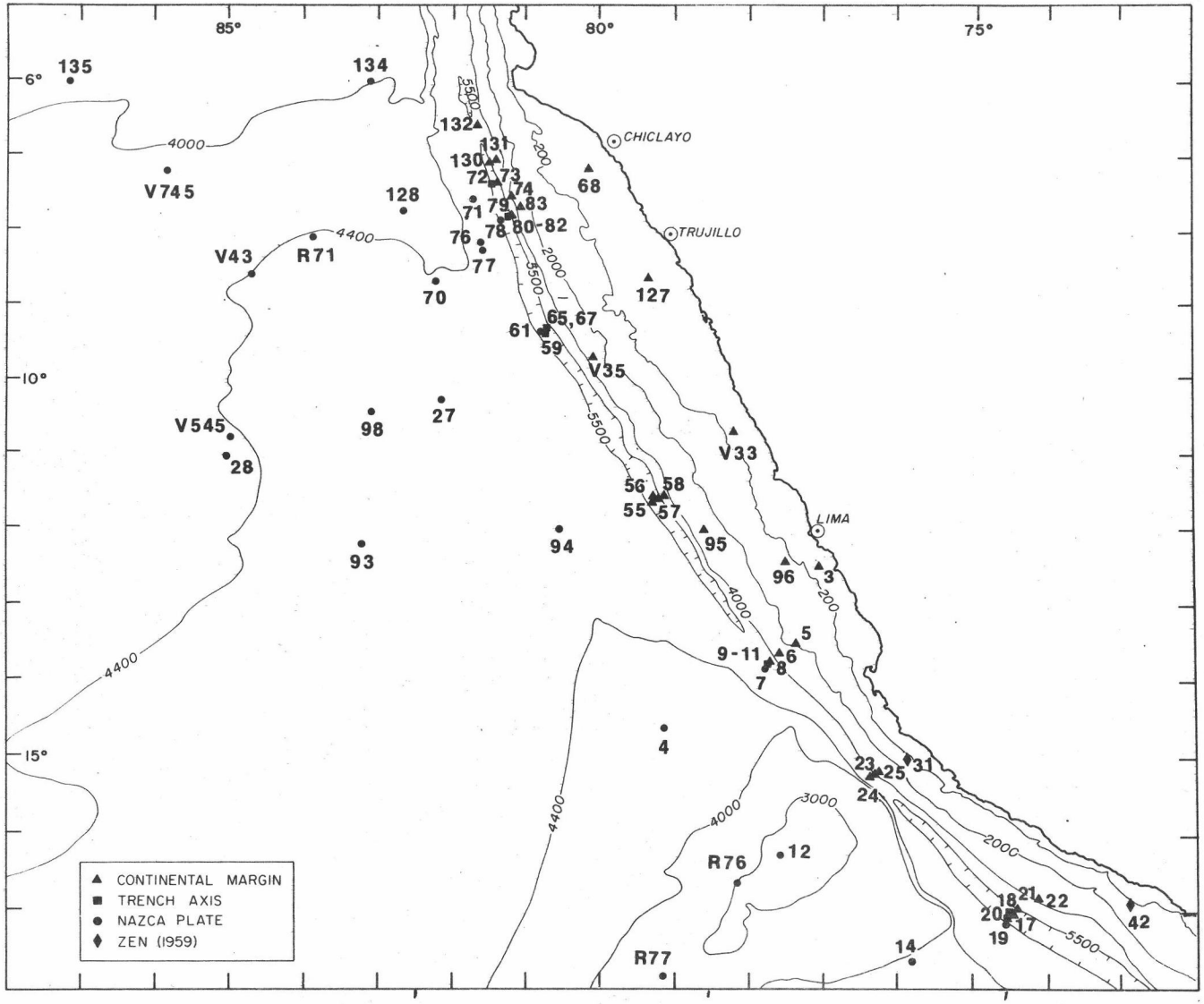

Figure 2. Core locations.

made of the <2μm fraction for each sample. Two slides were glycerol solvated and used for semi-quantitative calculations of clay mineral abundances, and one slide was ethylene glycol solvated to determine the degree of expansion of the smectite group of clay minerals. The values in Appendix II are the averages of the two glycerol treated slides. The sample from core Y71-6-5MG1 was split using a McManus splitter (McManus and others, 1966). One split was saturated with Mg, the other with K. Both samples were exposed to various heat treatments and organic solvants (Weaver, 1956; Hayes, 1973). Clay minerals were identified using charts and graphs found in Brown (1962) and Grim (1968), and semi-quantitative abundances were calculated using the weighting factors of Biscaye (1965). No attempt was made to distinguish polymorphs.

All samples were X-rayed on a Norelco Philips diffractometer with instrumental settings as follows: CuKα radiation, 35kV, 30 mA, 1° scatter and divergence slits, and 0.003 mm receiving slits. The scan rate for the clay slides was $\frac{1}{2}$° 2θ per minute between 3 and 20° 2θ, to resolve the principal peaks of the major clay minerals, and 1/8° per minute between 23.95 and 25.55° 2θ, to resolve kaolinite from chlorite.

Peak areas were measured with a polar planimeter. The mean differences between the duplicate samples were: 3.1% smectite and mixed-layer clays, 3.3% illite, 1.7% kaolinite, and 1.8% chlorite.

Characterization of Mixed-Layer Clays

Mixed-layer clays were found in several continental margin cores off Peru (Figure 4, Appendix II). Zen (1959) also reported mixed-layer clays in this area, but his data suggest they are interlayered smectite-illite clays. The only mixed-layer clays found in this study of sediments off Peru were smectite-chlorite intergrades.

The mixed-layer clays in this study are characterized by their behavior after Mg and K saturation, and various combinations of heating temperatures and organic solvants. They closely resemble clay minerals from the Pacific Ocean described by Oinuma and others (1959) and Powers (1957). If Mg saturation and glycerol solvation were the only tests performed on these samples, they would be termed montmorillonite of low crystallinity (Biscaye, 1965).

Typical mixed-layer clays off Peru (e. g., the surface sample from core Y71-6-5MG1) produce a broad band on diffractograms between 14 and 20 Å after Mg saturation and glycerol solvation. They lack resolvable higher order basal reflections and hybrid peaks in oriented mounts and display a resistance to collapse after K saturation and heating to 300° C (Figure 3). The 10 Å peak intensity relative to the 7 and 14 Å peak intensities did not increase after K saturation, which suggests that vermiculitic interlayers are not present. In some of the samples, ethylene glycol expands the structures to only 16.3 Å,

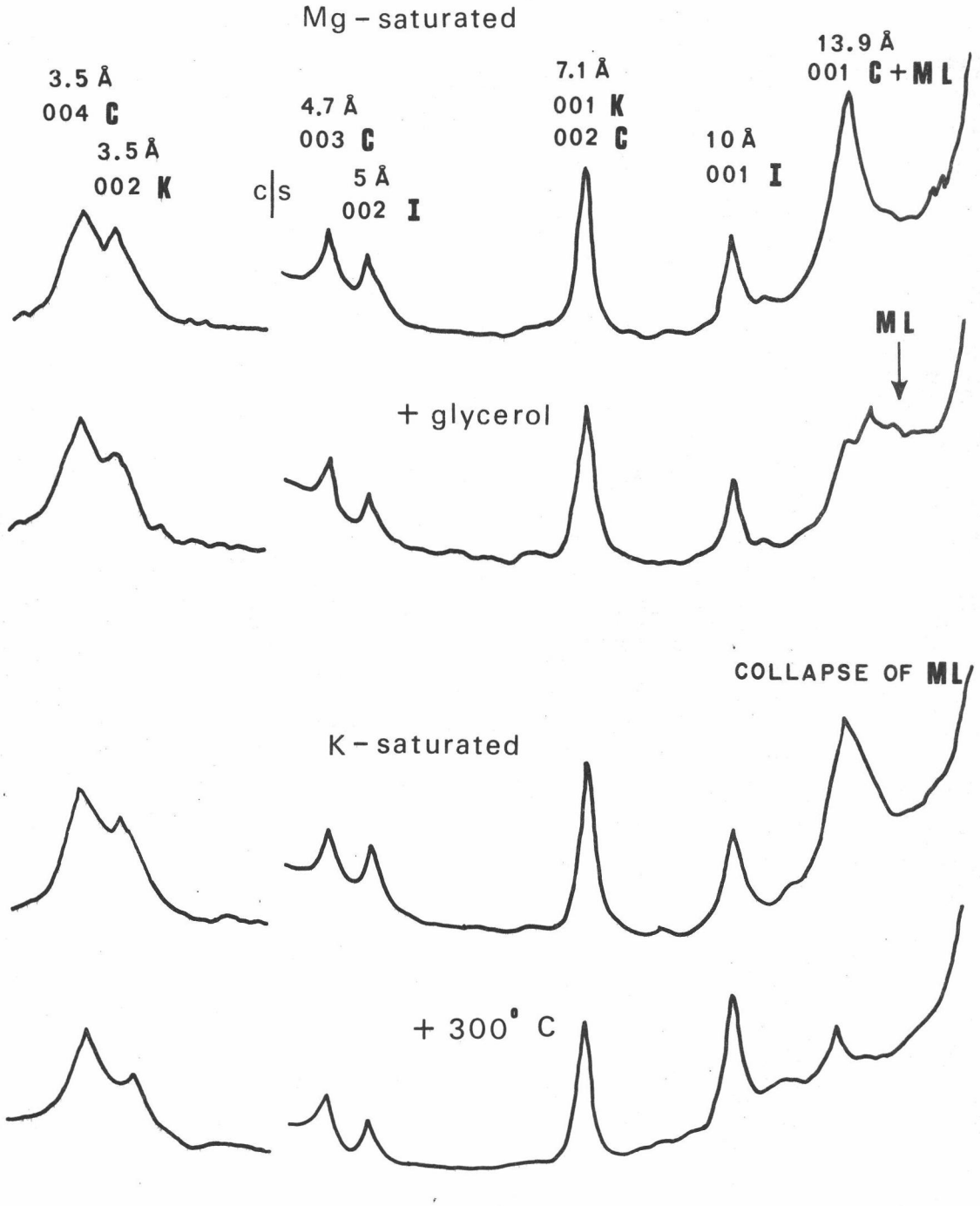

Figure 3. X-ray diffraction properties of the mixed-layer clay. ML = mixed-layer clay; I = illite; K = kaolinite; C = chlorite. Basal spacing (001) in Ångstroms. C/S = scale change.

which is less than expected for normal smectites.

Rather than indicating poor crystallinity (low valley to peak height ratio), these properties suggest structural similarities to the intergrade smectite-chlorite clay minerals commonly found in soils (Jackson, 1963) and recently synthesized in the laboratory (Carstea, 1967). These mixed-layer clays also have been termed swelling chlorites (Stephan and MacEwan, 1951), chloritized montmorillonite (Sawhney, 1958), and intergradient chlorite-expansible silicates (Dixon and Jackson, 1962). Carstea (1965, 1967) in a series of experiments was able to form hydroxy Al, Mg, and Fe interlayers in an American Petroleum Institute standard montmorillonite which had X-ray diffraction properties similar to the mixed-layer clay found off Peru. While the exact nature of the interlayer material is not indicated by the simple tests described here, hydroxy Al, Mg, or Fe interlayers in a smectite-like matrix are entirely possible. At least two authors (Rich, 1965; Carstea, 1967) believe that hydroxy Mg interlayers may be important in deep-sea sediments.

Other Techniques

Calcite and dolomite were determined by X-ray diffraction using a ThO_2 spike, which provides two precisely known peaks on either side of the calcite 101 and dolomite 104 peaks. Charts presented in Chave (1952) gave the percentage of Mg in the calcite structure.

Organic carbon and calcium carbonate determinations were made with a LECO induction furnace on duplicate samples from the same intervals as the clay samples. Carbon values that differed by more than 1% were repeated.

Paleontological Standards

The Radiolarian stratigraphy used here is based primarily on Hays (1970) and Berggren (1972). As discussed in Kulm and others (1974), the ages are based on the extinctions of four species:

Stylatractus universus 0.4 m.y.b.p.

Lamprocyclas heteroporous 2.0 m.y.b.p.

Stichocorys peregrina 2.7 m.y.b.p.

Stichocorys delmontensis 6.0 m.y.b.p.

Late Quaternary species were found most often and they resembled closely those described in surface samples by Dinkelman (1973, 1974) and Nigrini (1971). Only one surface sample was older than Quaternary, HIG Station 135 (late Miocene). With the exception of the Pliocene carbonate section in core Y71-6-24P (Kulm and others, 1974) and possibly the dolomite in core Y71-6-6P, none of the subsurface samples was older than 2 m.y.

SURFACE DISTRIBUTION OF CLAY MINERALS AND ORGANIC CARBON

The distribution of clay minerals on the Nazca Plate and Peru margin is difficult to explain unequivocally because of the virtual absence of information on the clay mineralogy of Peruvian soils, the unknown composition of dust loadings or river input from South America, and the poorly understood subsurface oceanic circulation patterns. My main intentions in this section, however, are to show that there are regional differences in the concentrations of particular clay minerals and organic carbon, and to offer plausible explanations for these differences. In later sections the subsurface data will be interpreted with these regional differences in mind. As stated previously, the purpose of the sediment study is to characterize the marine deposits well enough to detect pelagic sediments on the lower continental slope off Peru.

Smectites

There are several interesting trends shown in the distribution of smectite (including mixed-layer clays; Figure 4). First, there is a strong concentration gradient between the continental margin and Nazca Plate from 6° to 14°S. Because Zen's (1959) upper continental margin cores 31 and 42 (Figures 2 and 4) lacked smectites and mixed-layer clays, the concentration gradient probably extends south to at

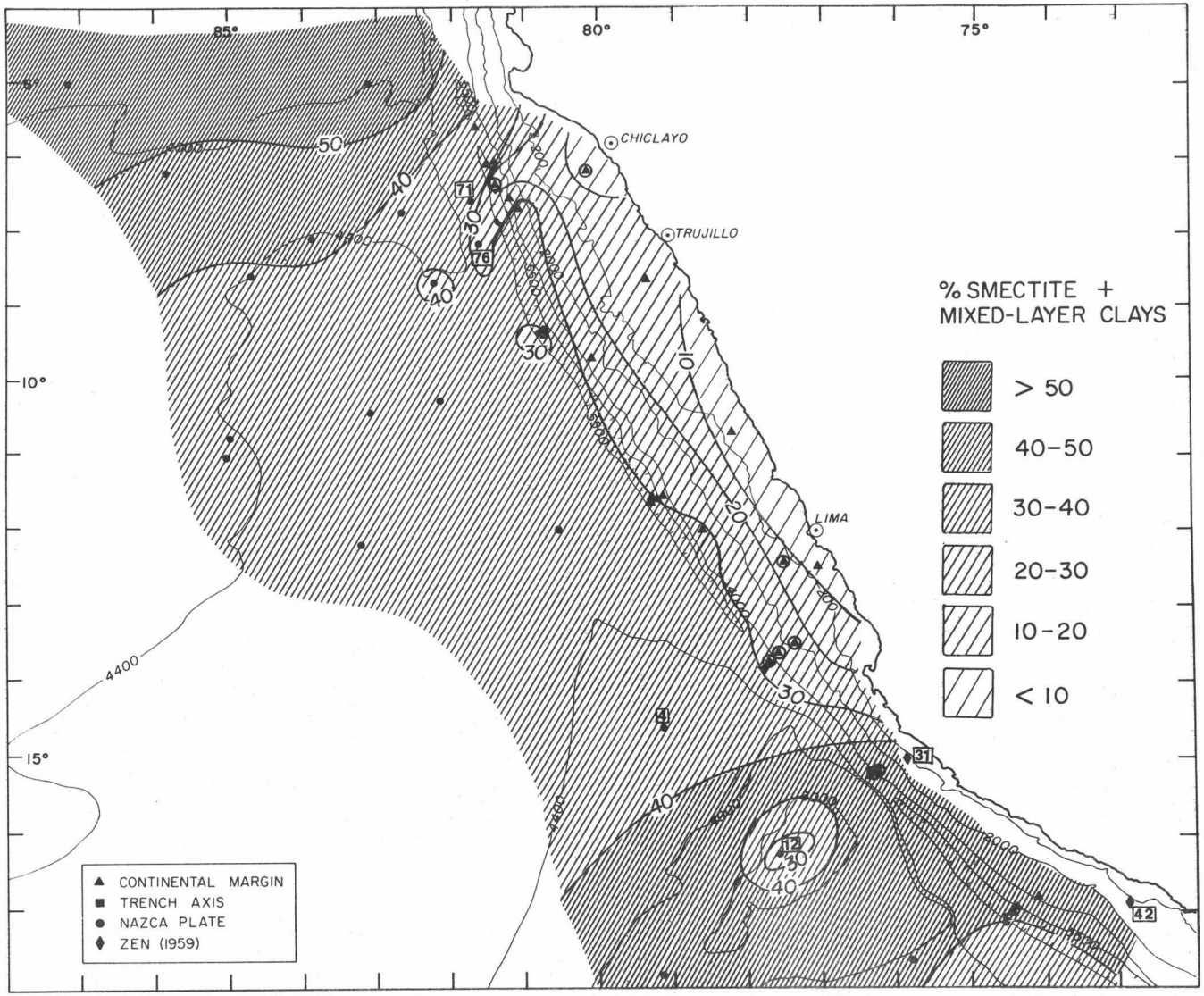

Figure 4. Surface distribution of smectite and mixed-layer clay. Circled symbols (▲) indicate sediments with mixed-layer clays. Cores discussed in text are indicated by numbers.

least 17°S. The dearth of smectite along the continental margin is unexpected because soils formed on volcanic terranes in arid climates usually are dominated by smectite and illite (Donoso, 1959; Grim, 1968; Besoain, 1969). Smectite-poor continental margin sediments also are unusual because volcanic ash is a common accessory of margin sediments (Zen, 1959; Rosato and others, 1973). Smectites completely dominate the <2μm fraction of partially altered ash layers from three cores (4, 12, and 71), which suggests that marine deposits of Andean volcanic ash apparently weather to smectites. Thus, either continentally-derived smectite is diluted by other clay minerals weathered from the coastal batholiths of Peru, or smectite, which is the finest grained of the clay minerals, is winnowed out of margin sediments or kept in suspension by strong coastal currents. Both phenomena may be occurring.

Another interesting feature of the surface distribution of smectite is the smectite-rich area near the Equator. The smectite concentrations in this region are greater than 50%, which agrees with the results of other authors. Griffin and others (1968) found > 70% smectite in the <2μm fraction of sediments from this region, and Heath and others (1974) found > 80% smectite in surface samples to the north of this region. Even though the surface sample from core 135 is late Miocene in age, it is wholly smectite and is probably

representative of Quaternary sediments at that site. Since smectite can be formed within the ocean basins or derived from the continent, smectite enrichments in this area are not unexpected. This area is close to the East Pacific Rise and Bauer Deep (Figure 1), where iron-rich smectites are forming (Kendrick, 1974; Eklund, 1974), and to smectite sources in Ecuador (Heath and others, 1974) and northwestern Peru (S. B. Weed, written communication).

The fairly constant concentration of smectite in the Peru Basin is noteworthy. It may result from a dynamic balance between the rate of oceanic and continental input of smectite to the basin.

The distribution of smectite south of 14°S is somewhat different from that north of 14°S. The concentration gradient between continental margin and Nazca Plate sediments, while probably present as mentioned previously, is shifted markedly towards the shore. Both Nazca Plate and lower continental margin surface sediments contain roughly equivalent amounts of smectite. Except for one sample on the northeastern end of the Nazca Ridge (12-1; Figure 4), values on the ridge are between 40 and 50%. One possible reason for the increased smectite concentrations south of 14°S is the greater exposure of recent volcanic debris south of about 14°S (see Mapa Geologico Generalizado del Peru, Servicio de Geologica y Mineria, 1969). The high concentrations could also be due to deposition from smectite-rich, northward flowing Subantarctic water. The low smectite content in

sample 12-1 is probably due to dilution by continentally-derived clays.

One final trend in the smectite distribution is the prominent lobe of smectite-poor sediment extending seaward from the present trench axis at 7° to 8°S (Figure 4). A northeastern source is indicated. The continental slope in this area is cut by several submarine canyons (Prince, 1974) and the rivers are relatively large for this coastal region. Since surface currents flow in a direction opposite to the trend of the lobe and since there is a topographic low between core 76 and the coast, mid-water transport is implied. Another possibility is that the sediment may be the fine-grained tail (pelitic interval) of a turbidite, representing sediments displaced from the continental margin.

Mixed-Layer Clays

The restriction of smectite-chlorite mixed-layer clays to two areas landward of the trench is intriguing (Figure 4). There are several possible sources of mixed-layer clay:

(1) chemical alteration during pre-treatment

(2) halmyrolysis of oceanic rocks

(3) weathering of continental rocks

(4) diagenetic alteration of chlorite or montmorillonite on the sea floor.

Judging from the studies of Carstea (1967) and Harward and others (1962), chemical pre-treatment, especially the Na citrate-dithionite and Na_2CO_3 treatments, would reduce the number of interlayers in mixed-layer clays. Furthermore, it is unlikely that the pre-treatments would affect only continental margin clay minerals.

Halmyrolysis (submarine weathering) of basalt, as proposed by Rex (1967), probably did not contribute much mixed-layer clays to the continental margin. If this process occurs, it should be more prevalent on the Nazca Plate than on the continental margin. The sediments of the Nazca Plate, however, contain well-crystallized smectite, but no mixed-layer clays.

While smectite-chlorite intergrades are common in soils (Jackson, 1963; Carstea, 1967), including those found on volcanic ash (Chichester and others, 1969; Singleton, 1966), there is no direct link between continental sources of smectite-chlorite mixed-layer clays and the marine environment except through a diagenetic intermediary (e.g., Powers, 1957). It would be difficult to trace mixed-layer clay from the continent without detailed sampling.

There is no data that would indicate the mixed-layer clays are forming in the sediments off Peru by diagenesis, though the high organic content of sediments with mixed-layer clays (Appendix II) may be a factor that encourages diagenesis. On one hand, the sediments in cores 55, 56, 57, and 58 had mixed-layer clays at the bottom

but not at the top. Several samples at intermediate depths in the cores would be required to determine if there was a gradual increase in the degree of interlayering with depth. On the other hand, three samples from core 5 (top, middle, bottom) contained mixed-layer clays, with very little difference in the relative proportion of mixed-layer clay with depth (Appendix II).

Illite

Illite concentrations in the surface sediments generally decrease with increasing distance from the continent (Figure 5). The highest concentrations occur on the shelf at 11°S (core V33). The lowest concentrations occur on the Nazca Ridge (core R77) and near the Equator (core 135). The illite content is fairly constant across the Peru Basin, ranging from 40 to 47%. There is a concentration gradient from northeast to southwest on the Nazca Ridge.

In the Northern Hemisphere illite is thought to be transported mainly by the winds. The highest illite concentrations occur beneath the mid-latitude jet stream and on topographic highs (Griffin and others, 1968). Rivers, such as the Mississippi and Amazon, also make large contributions of illite to the ocean.

The distribution pattern of illite off Peru has features indicative of both aeolian and fluvial inputs. Dispersal in the water column from local sources is shown by the seaward decreasing illite

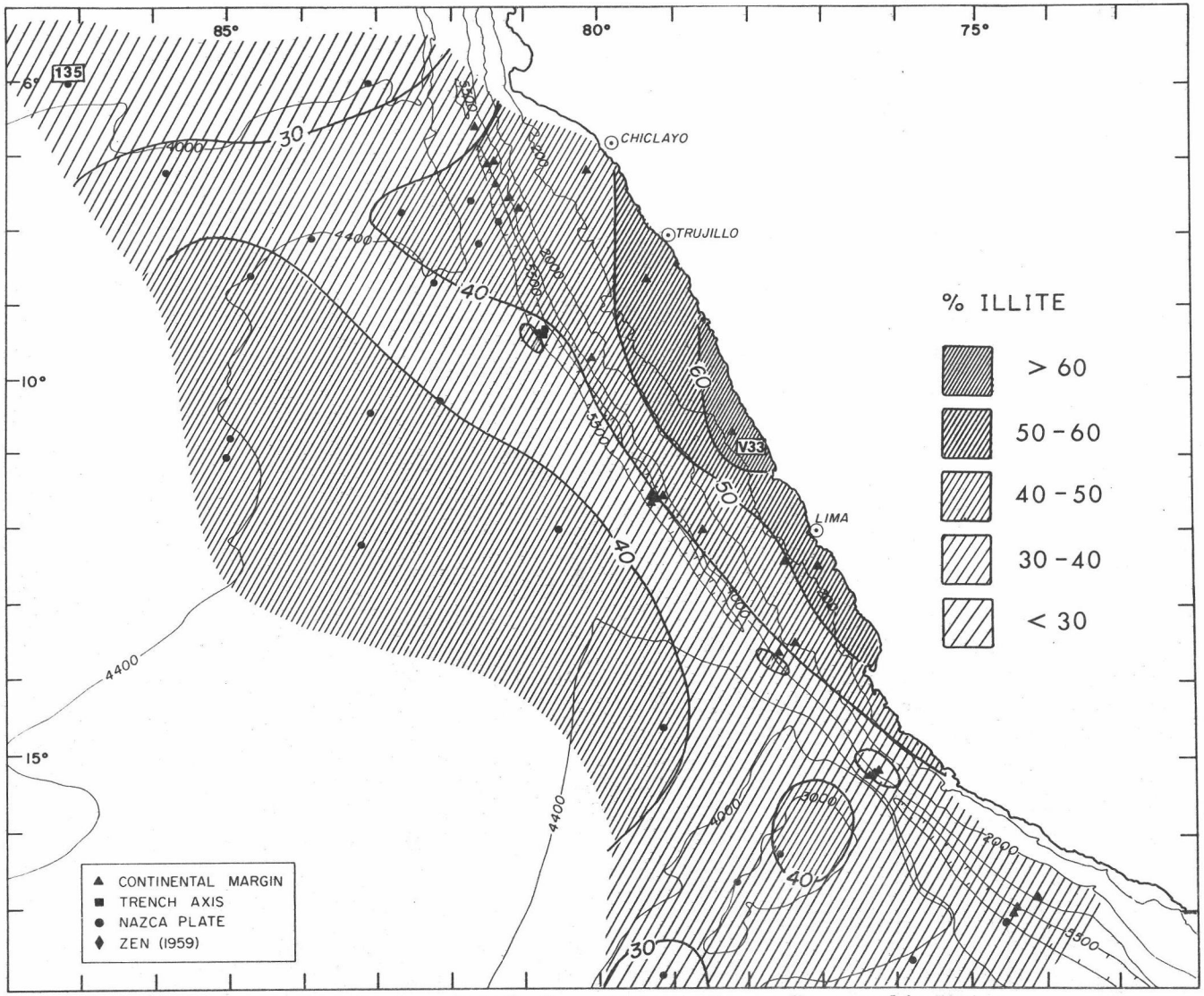

Figure 5. Surface distribution of illite. Cores discussed in text are indicated by numbers.

concentrations on the continental shelf, and atmospheric transport is indicated by the relatively high concentrations on topographic highs.

Because of the scarcity of Peruvian shelf samples, it cannot be definitely shown that particular rivers are the source of illite. The high illite values found near 11°S suggest that this area may be a source of illite-rich sediments. Near the Equator illite values are low because there are few sources of illite in northwestern South America (Heath and others, 1974).

The decrease in illite values to the southwest on the Nazca Ridge is a function of increasing distance from the continent. Because there are low concentrations of illite in the trench sediments between the continent and the Nazca Ridge, and high concentrations on the northeastern end of the Nazca Ridge, aeolian dispersal of illite is indicated. Low concentrations of illite in the trench are probably due to dilution by materials carried by the deeper parts of the water column.

Chlorite

The distribution of chlorite in surface sediments is the result of hemipelagic sedimentation. Concentrations generally decrease with increasing distance from the continent without regard to topography (Figure 6). Highest concentrations occur on the continental shelf near 13°S (31%), and the lowest concentrations occur on the

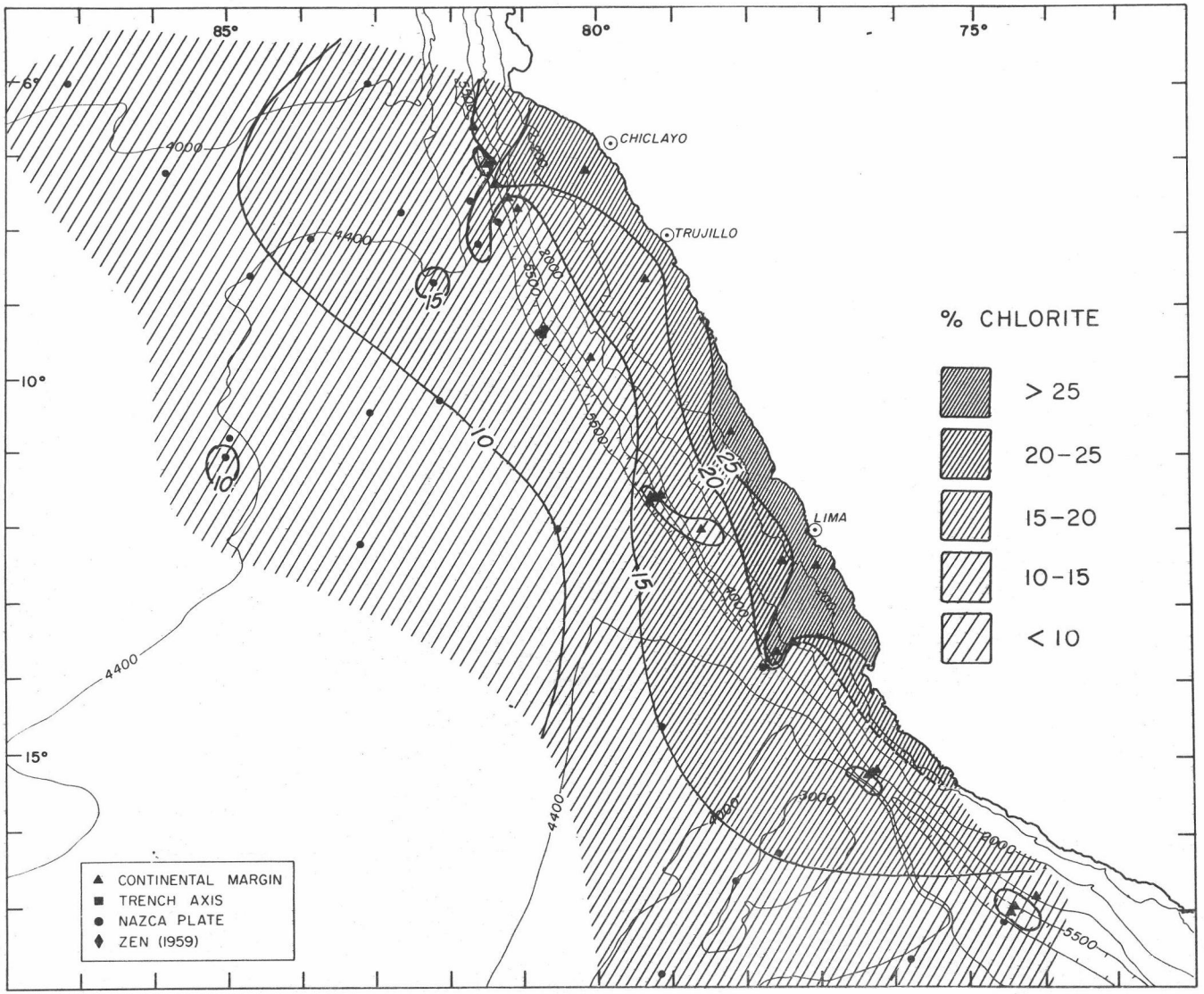

Figure 6. Surface distribution of chlorite.

Nazca Plate (<10%). In general, the distribution of chlorite is the inverse of smectite. The chlorite-rich sediments seaward of the trench at 7°S, like the lobe of smectite-poor sediments, indicates a source area to the northeast. There is also a southward-trending lobe of chlorite-rich sediments off Lima, Peru.

The metamorphic terranes associated with the Upper Cretaceous to Lower Tertiary batholiths (tonalite, granodiorite, diorite and granite) of coastal Peru are possible sources of the chlorite. Most of these rocks crop out in the coastal region between 8° and 16°S.

Kaolinite

Kaolinite concentrations in surface sediments is quite similar to those of chlorite. Tongues of kaolinite-rich material extend southward from near Lima and westward from Chiclayo, indicating possible sources in these areas (Figure 7). Kaolinite contents generally decrease seaward, but concentrations on the northeastern end of the Nazca Ridge are slightly lower than concentrations to the north and south.

Because kaolinite values are low on the Nazca Ridge, dispersal of kaolinite by winds is not indicated. The lobes of kaolinite-rich sediments extending seaward of Lima and Chiclayo suggest dispersal in the water column to the south and west, respectively. The fairly low and constant concentrations of kaolinite across the Peru Basin

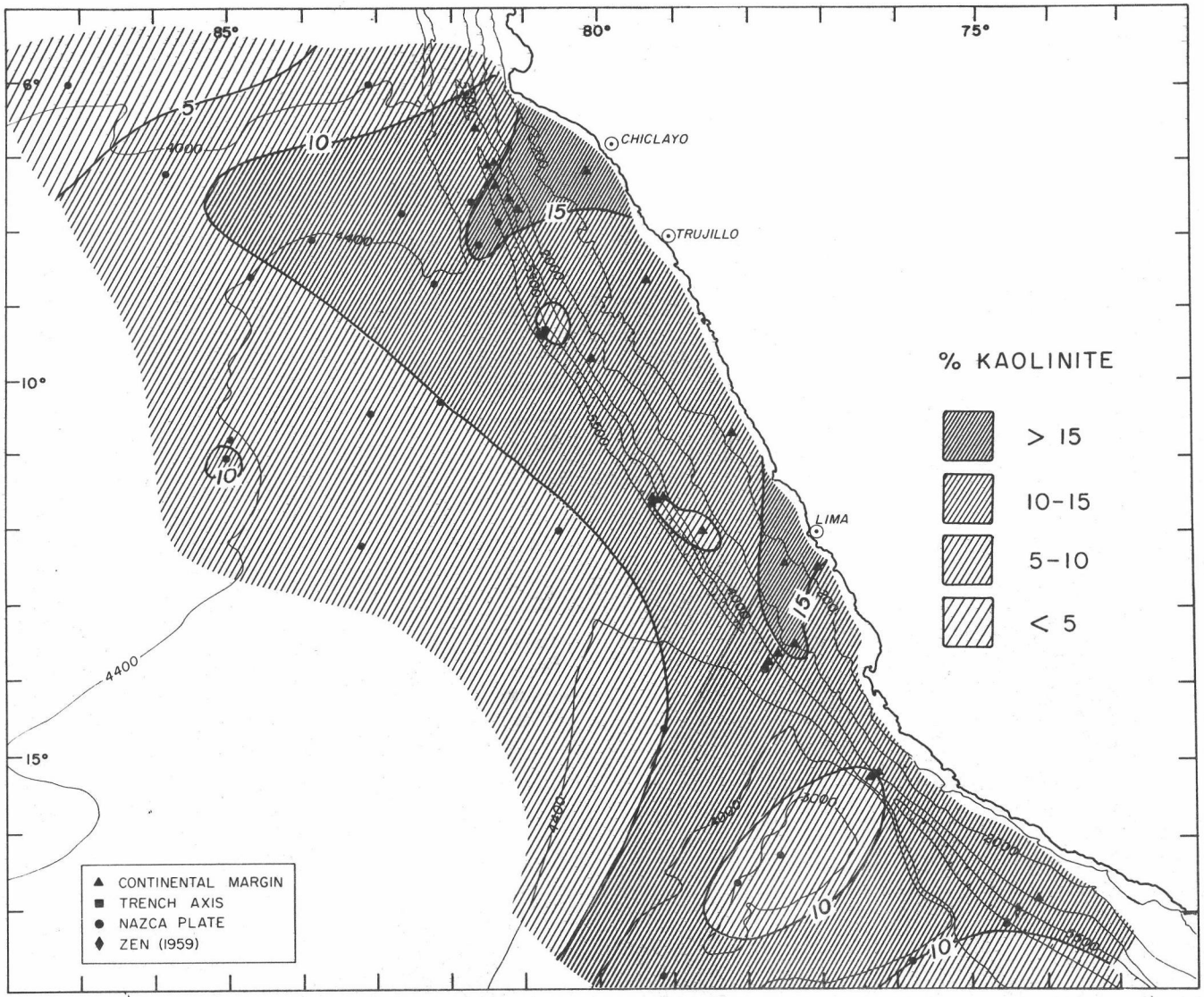

Figure 7. Surface distribution of kaolinite.

imply slow hemipelagic sedimentation in these areas. Because arid and semi-arid climates now prevail in Peru west of the Andes (McGinnes and others, 1968; Suzuki, 1973), and because kaolinite is thought to be formed under tropical (intense) weathering conditions, this clay mineral is probably derived from older sedimentary rocks in western Peru.

Organic Carbon

The distribution of organic carbon in surface sediments is shown in Figure 8. Organic carbon values generally decrease away from the continent. Isopleths of organic carbon content broaden as they approach the Equator. There is also a seaward projection of moderately high values (2-3%) over the northeastern terminus of the Nazca Ridge. The highest organic carbon values (7.5%) occur on the upper continental slope and shelf at about 13°S, just south of Lima. Anomalously low organic carbon contents (<1.5%) are found on the continental shelf in cores 68 and 127.

The various factors governing the amount of organic carbon in sediments have been discussed in Trask (1939) and Gross and others (1972). As discussed in Rosato and others (1974), the primary factor controlling the distribution of organic carbon in surface sediments off Peru is productivity; sediments below highly productive upwelled waters generally have significant amounts of organic carbon. The

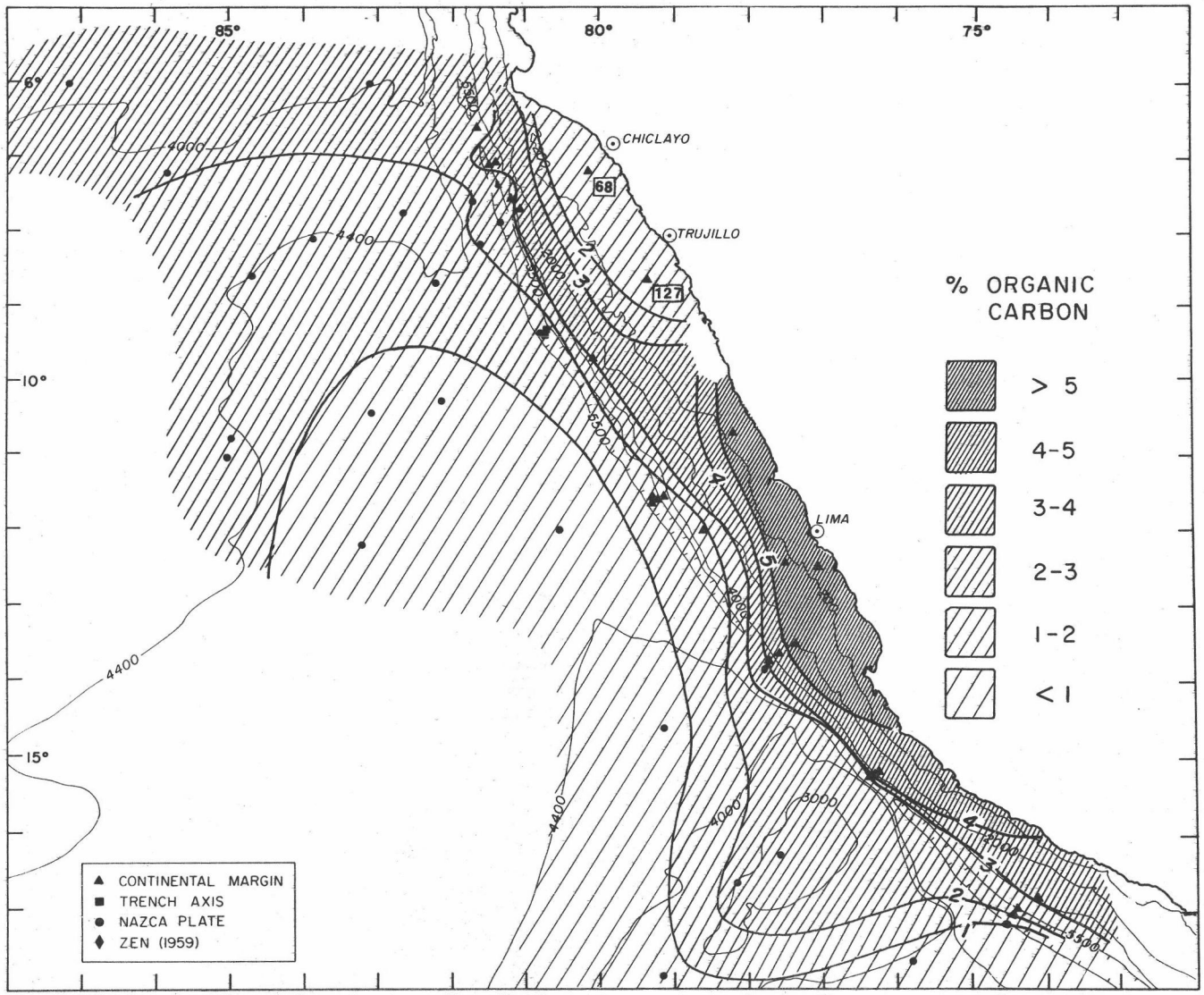

Figure 8. Surface distribution of organic carbon. Cores discussed in text are indicated by numbers.

anomalously low values on the continental shelf between 7° and 8°30'S are probably due to reworking by strong bottom currents; samples 68-1 and 127-1 had much higher percentages of sand than shelf samples to the south (V33-1 and 3-1). Enhanced preservation of organic matter within carbonate tests may lead to the moderate organic carbon contents of the northeasternmost Nazca Ridge samples. Smith and others (1971) have suggested that this is an area where currents converge, possibly leading to increased productivity and increased deposition of organic matter.

FACTOR ANALYSIS

Theory

In order to clarify the interrelationships of the clay mineralogy and organic carbon content, to identify possible source areas, and to create some quantitative basis for identifying displaced fine-grained sediments, the clay mineralogy and organic carbon contents were submitted to Q-mode factor analysis.

This method of factor analysis constructs a linear mixing model involving a small number of end members with extreme compositions. In more statistical terms, the objective of factor analysis is to account for the variance in the data matrix. The resulting output is a series of maps which indicate the degree of similarity of each

sample to a theoretical end member (factor or vector). Each factor, if it is considered to be geologically meaningful by the operator, can then be given a name (e. g.: oceanic assemblage, continental assemblage).

The theory of Q-mode factor analysis as applied to geologic problems is discussed in greater detail in Imbrie and van Andel (1964) and Imbrie and Kipp (1971). The computer program which performs the analysis, CABFAC, is described in Klovan and Imbrie (1971), Sachs (1973) and Dinkelman (1974).

The technique used here proceeded in two steps. In the first step, the surface data were subjected to Q-mode factor analysis. The second step entered all the subsurface data, including the basal samples of lower continental margin cores taken on outcrops of acoustic basement, into the surface model by constructing a pseudo-factor matrix (i. e.; parafactor of Sachs, 1973). This second step is accomplished by the computer program THREAD. The second step does not construct a new set of factors, it simply multiplies the normalized raw data of the subsurface samples by the varimax factor score matrix from the CABFAC program. As shown below, this allows the recognition of displaced sediments.

Model Selection

Two geologically reasonable factor models can be constructed

from the data. One model consists of three factors and the other four factors (Figures 10 and 9). In the three-factor model, the data were entered as listed in Appendix II; that is, without any transformations. In the four-factor model, a percent range transformation was performed. This was done in order to give all the variables (smectite, mixed-layer clays, illite, kaolinite, chlorite, and organic carbon) equal weight, since without the transformation most of the variability is in the concentrations of smectite and illite.

The factors for each model are compared in Figures 9 and 10, which shows the scaled varimax factor scores. In both models, about 99% of the variance is explained by the factors.

The four-factor model consists of an oceanic assemblage, continental assemblages A and B, and an authigenic assemblage (Figure 9) that account for 59, 24, 11, and 4% of the variability, respectively. The model explains the data well; the average communality (sum of the squares of the varimax factor scores for each sample) was 98.5%. None of the communalities were lower than 95.4%. However, little additional information is gained by using a four-factor model rather than a three-factor model. One thing that the four-factor model shows that is not evident in the three-factor model is a significant increase in oceanic factor (1) loadings and a significant decrease in continental factor (3) loadings with increasing depth in core 4 (Figure 11). This implies that the continental influence

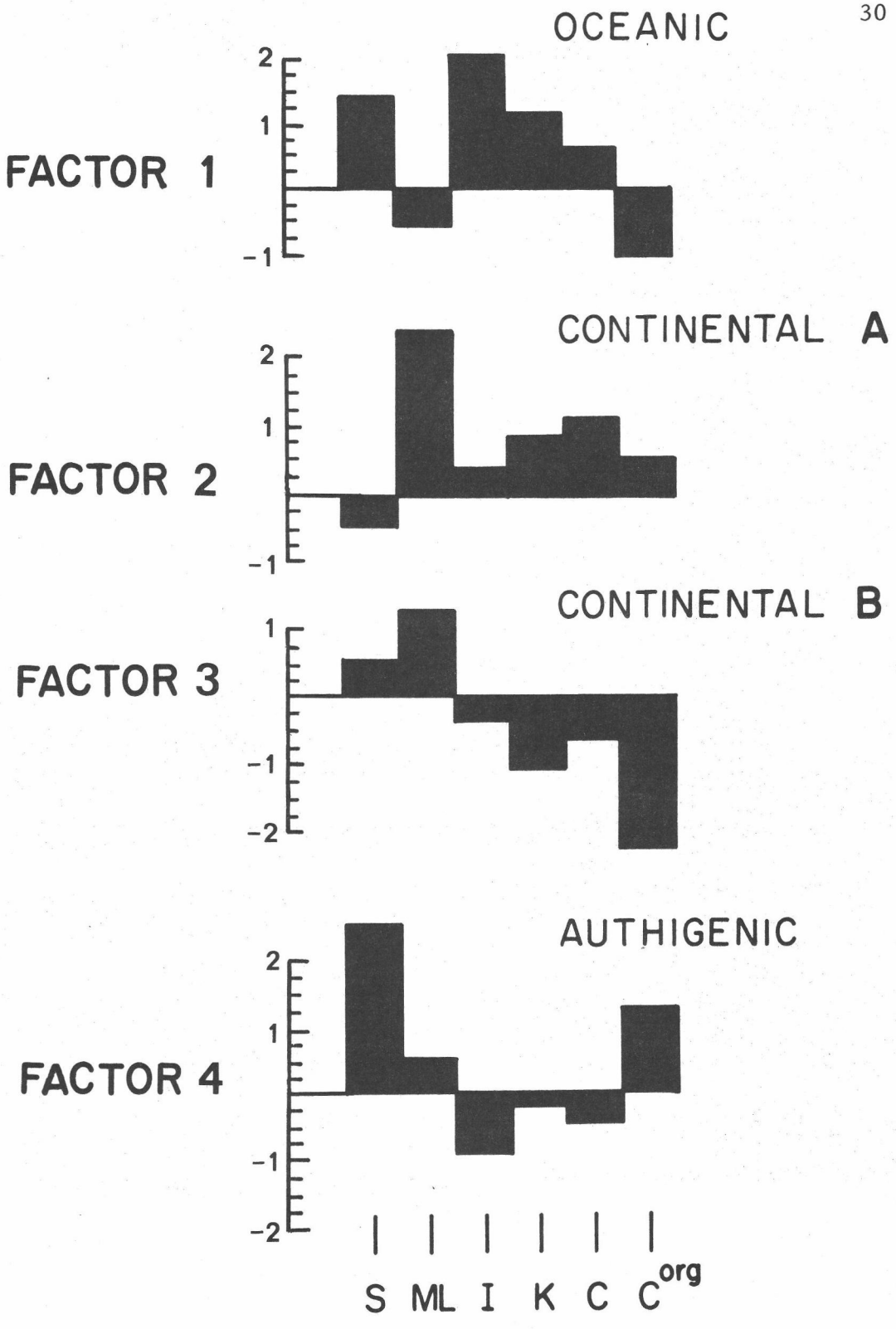

Figure 9. Scaled varimax scores, four factor model. S = smectite; ML = mixed-layer clay; I = illite; K = kaolinite; C = chlorite; C^{org} = organic carbon.

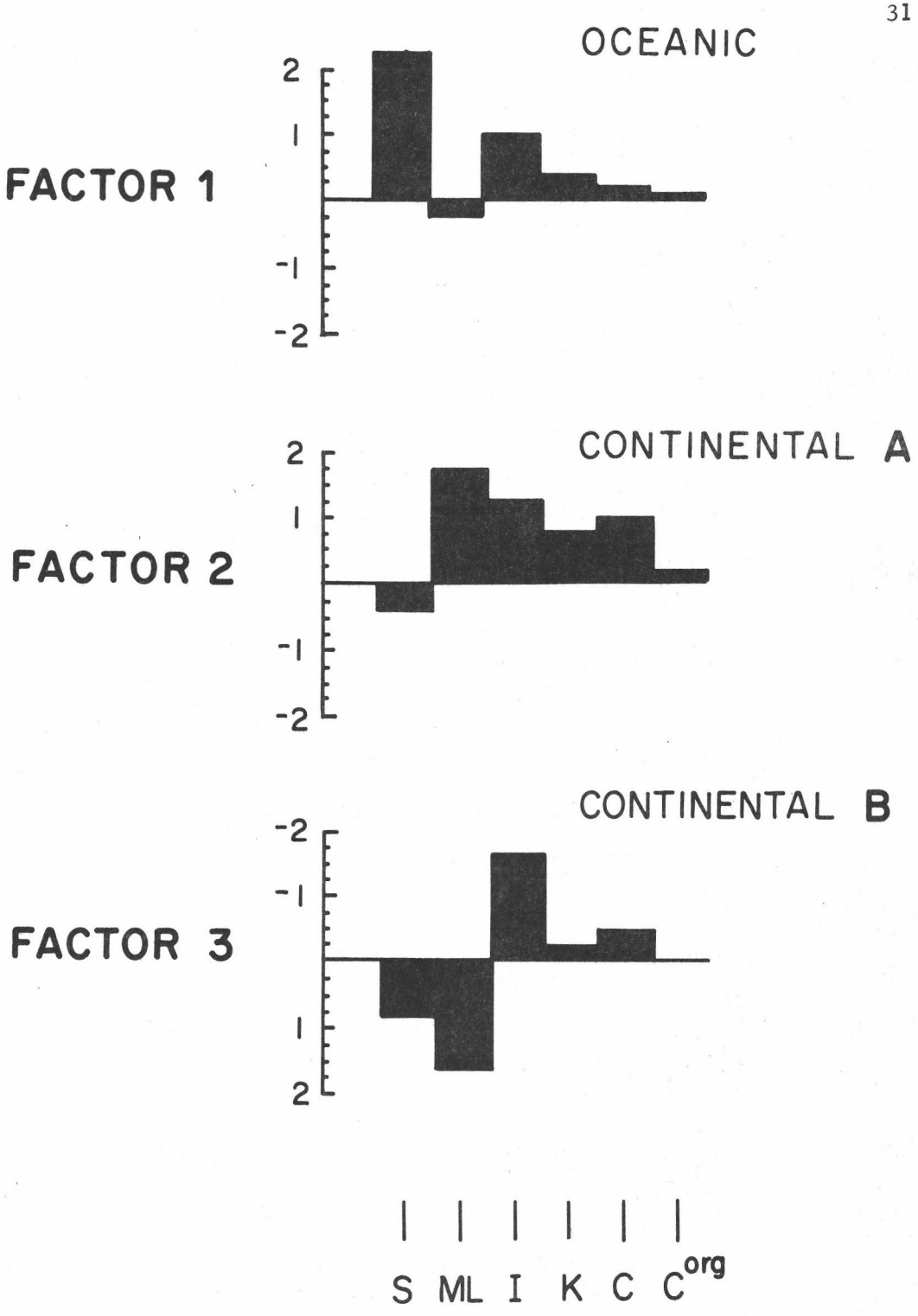

Figure 10. Scaled varimax scores, three factor model. Factor 3 scores are inverted. Same abbreviations as Figure 9.

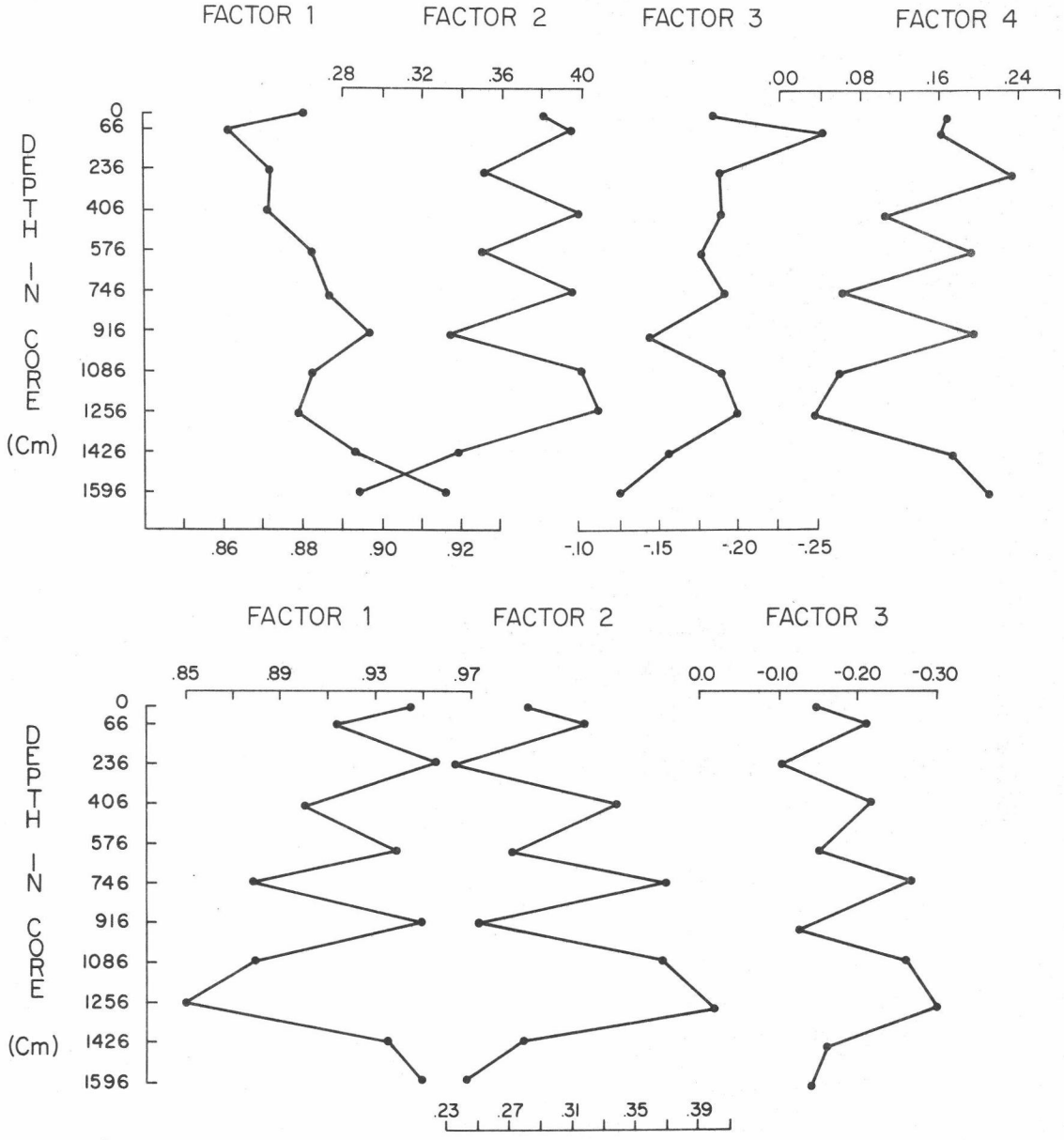

Figure 11. Change in factor loadings with depth in core 4. The upper diagram is for the four factor model, the lower diagram is for the three factor model. Correlation coefficients (factor loading vs. depth in core) for the upper diagram are 0.76, -0.42, -0.61 and -0.18 for factors 1 through 4, respectively. In the lower diagram, the correlation coefficients are -0.19, 0.10, and 0.21 for factors 1 through 3, respectively.

at a particular spot on the Nazca Plate will gradually increase as the Nazca Plate and the South American Plate converge.

In the three-factor model, the oceanic assemblage, continental assemblage A, and continental assemblage B account for 65, 25, and 10% of the variability, respectively. Communalities for all samples were greater than 95.7%, with an average of 99.3% (Appendix III). Factor loadings (component of the varimax matrix for a particular factor at a particular sample) are listed in Appendix III. Because the three-factor model is simpler, further discussion will be restricted to it.

Factor Mapping

The three factors are compared in Figure 10. Factor 1 is termed the oceanic assemblage because it is dominated by smectite and subordinate illite and because factor loadings tend to increase away from shore. The areal distribution of factor 1 (Figure 12) resembles the surface concentrations of smectite (Figure 4). The sample with the highest oceanic factor loading (R77-1) is on the southwestern part of the Nazca Ridge (Figure 12). Lowest values are found on the continental margin opposite the Nazca Ridge. Sediments on the northeastern end of the Nazca Ridge as well as on the continental margin have lower oceanic factor loadings because they have higher organic carbon contents and higher proportions of

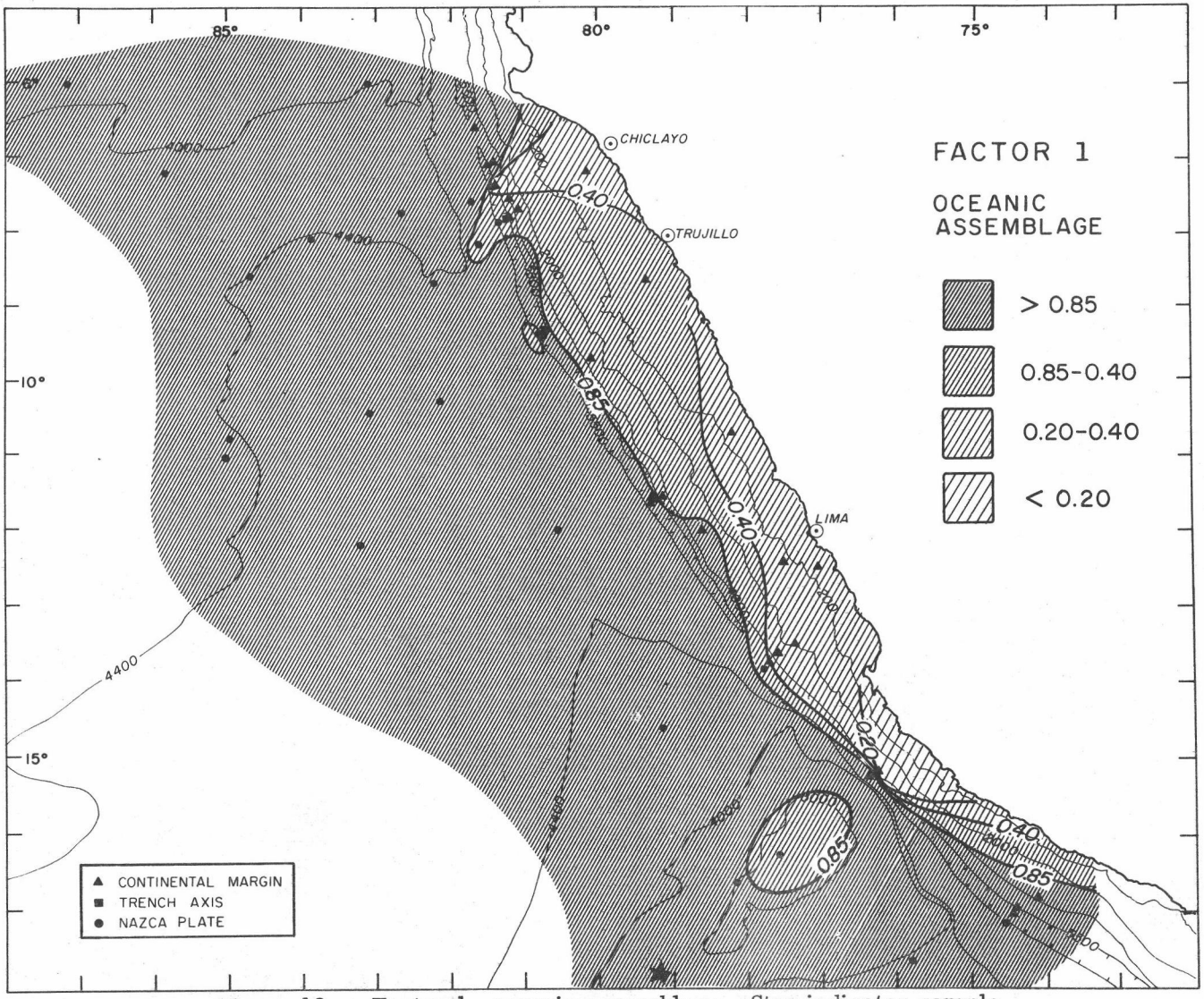

Figure 12. Factor 1, oceanic assemblage. Star indicates sample with highest factor 1 loading (R77-1).

continentally-derived clays. The illite component of this factor probably represents aeolian illite, while the illite component of factor 2 probably represents fluvial illite.

Factor 2 is termed continental assemblage A because it is comprised of detrital clay minerals (illite, Kaolinite, and chlorite) and mixed-layer clays. Figure 13 shows that the factor loadings for factor 2 decrease away from shore. Sample 23-1, on the middle continental slope at 15°S, has the highest factor 2 loading. The tongue of high factor loadings that extends seaward of the trench at 7°S, like the surface distributions of chlorite and kaolinite (Figures 6 and 7, respectively), indicates a sediment source to the northeast. A major source for this assemblage may be the coastal Arequipa Massif (sillimanite and garnet gneiss, K-feldspar-rich granite and pegmatite; Cobbing and Pitcher, 1972), which lies directly opposite the Nazca Ridge.

Factor 3 is termed continental assemblage B. It is characterized by an abundance of illite and an absence of smectite and mixed-layer clays. Consequently, a map of factor 3 loadings resembles the distribution of illite (Figure 5). Sample V33-1 on the continental shelf (Figure 14) has the highest factor 3 loading. Because this vector is in negative space, values increase away from shore.

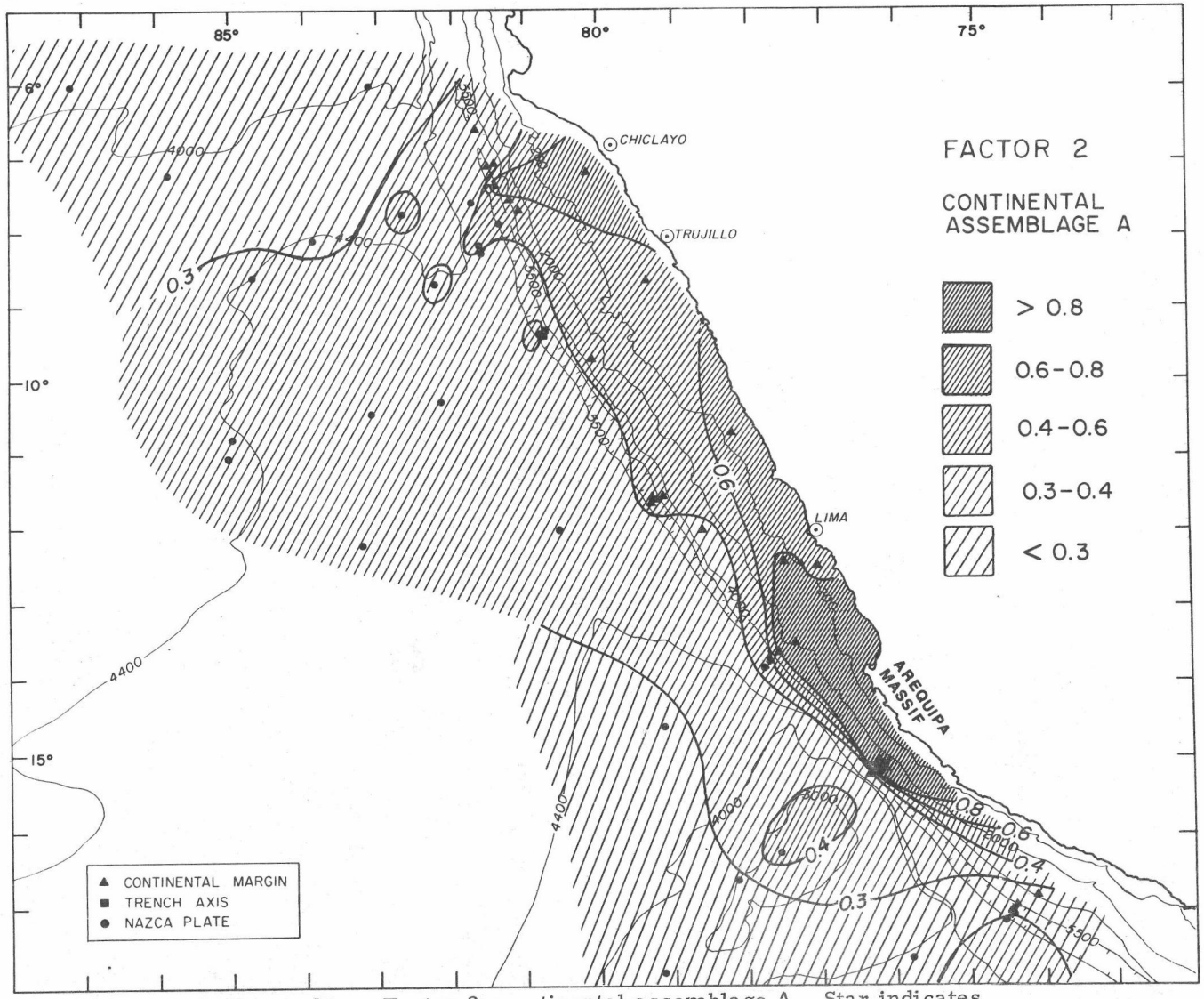

Figure 13. Factor 2, continental assemblage A. Star indicates sample with highest factor 2 loading (23-1).

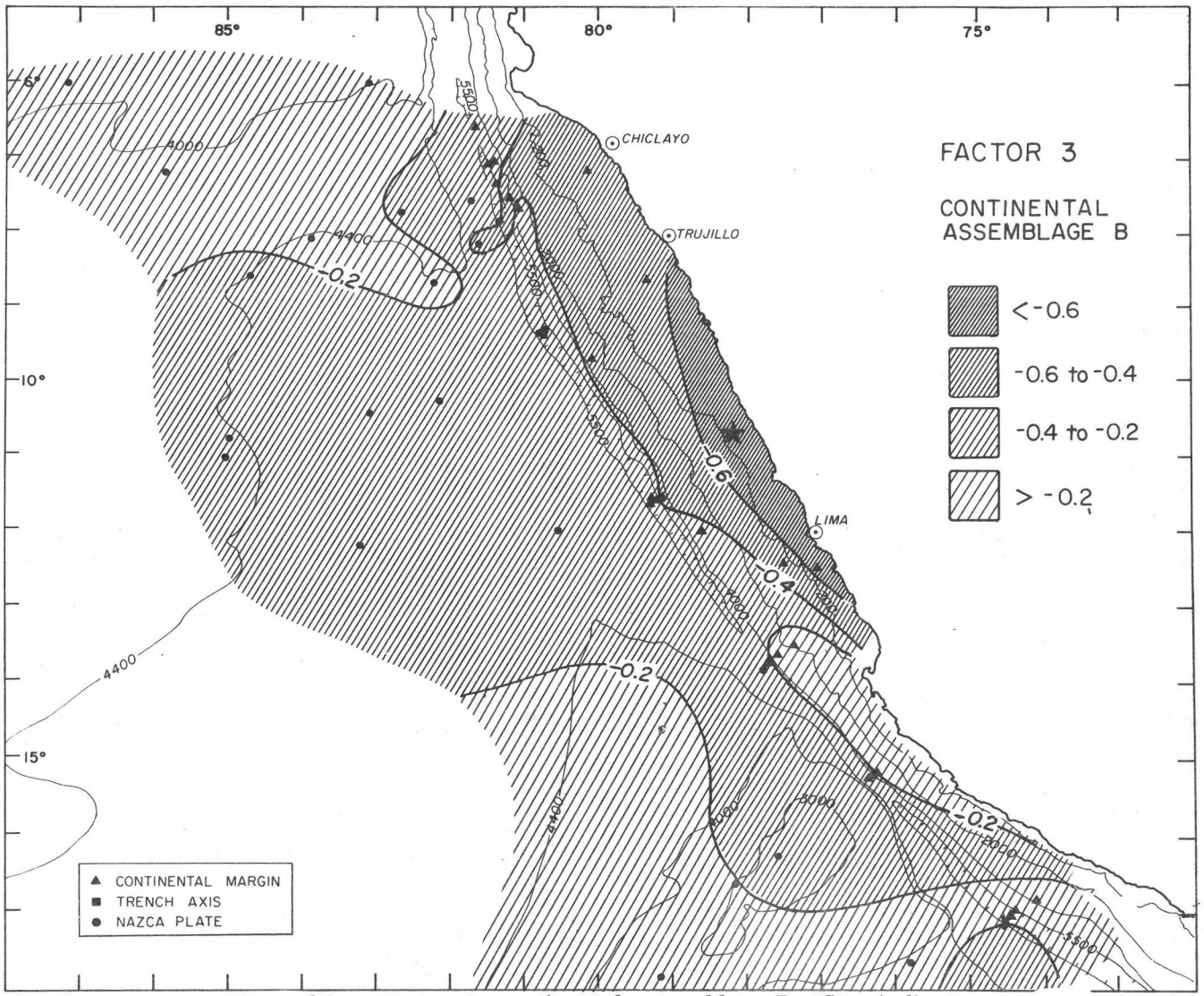

Figure 14. Factor 3, continental assemblage B. Star indicates sample with highest factor 3 loading (V33-1).

Factor Dominance in Surface Sediments

The dominant factor in all Nazca Plate surface sediments is factor 1 (oceanic assemblage; Figure 15). Except for core 127, where all three factors are equally important and core V33, where factors 2 and 3 (continental assemblages A and B) are equally important, the dominant factor in upper continental margin (<2000 m) sediments is factor 2. Lower continental margin sediments are more variable; they are either dominated by factor 1 or factor 2. Factor 3 does not dominate any of the surface or subsurface sediments.

The boundary between oceanic and continental sediments (as defined by dominance of factors 1 and 2) parallels the continental margin. In most areas, the sampling density is not great enough to precisely define this boundary. The boundary, however, lies higher on the continental margin to the north and south of the Nazca Ridge than it does opposite of the Nazca Ridge. The boundary is particularly well-defined between 14° and 15°S, where it lies approximately at the base of the steep continental slope. The boundary probably occurs on the upper continental slope northeast of core 22 because: (1) Zen's (1959) core 42 apparently lacks smectites and mixed-layer clays and contains illite, kaolinite and chlorite, (2) core 42 lies within the region expected to have from 2 to 4% organic carbon (see Trask, 1959; Rosato and others, 1974), and (3) surface sediments from cores with

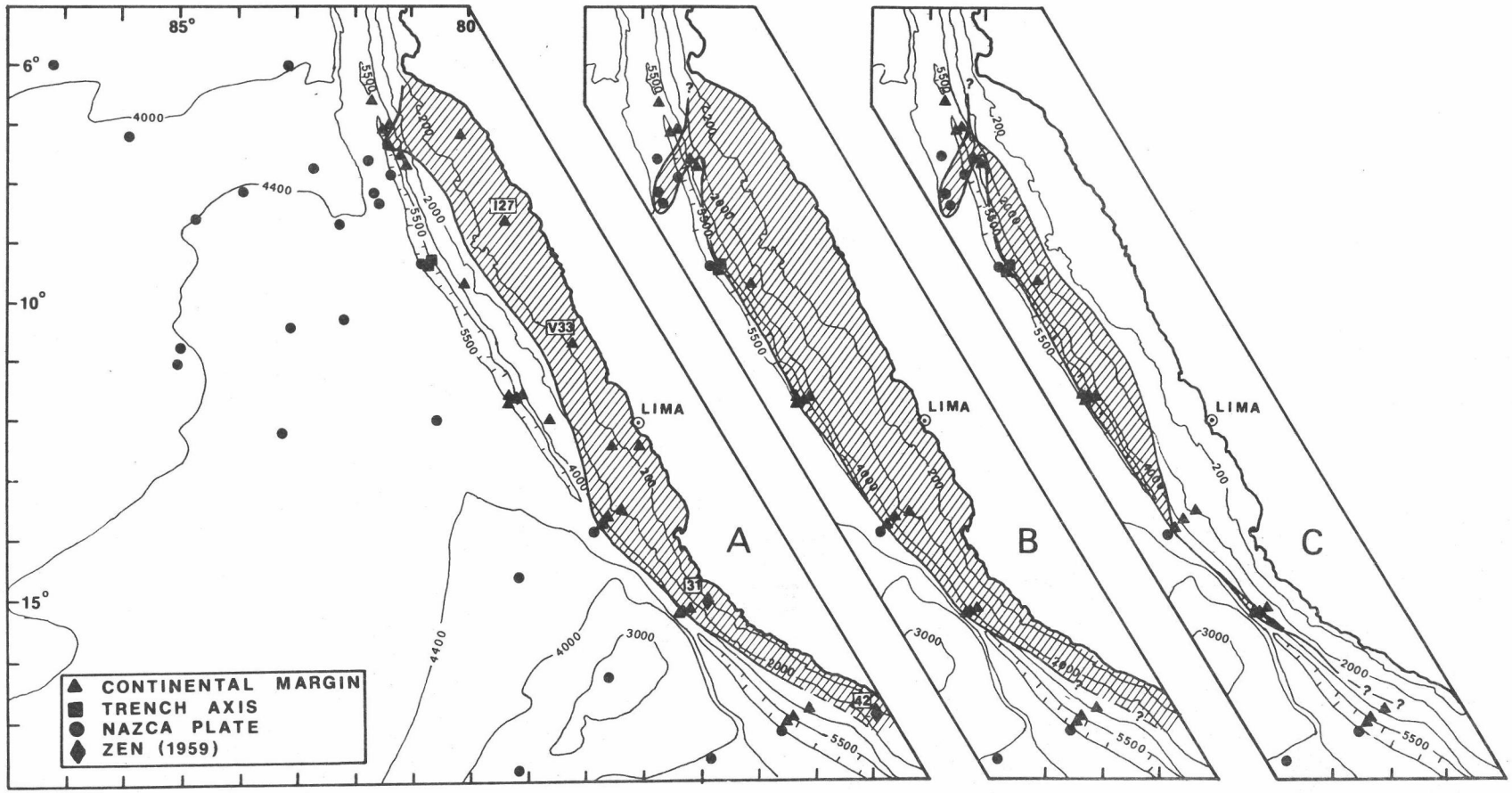

Figure 15. Factor dominance in surface and subsurface samples. A. Present location of the boundary between oceanic factor dominated (white pattern) and continental factor dominated (line pattern) surface sediments. B. Boundary earlier in the Quaternary. C. Difference between early Quaternary and late Quaternary boundaries.

similar compositions (core V33) are dominated by factors 2 and/or 3. Between 8° and 13°S, and at 17°S, the continental slope is not as steep and the oceanic assemblage occurs higher on the slope.

The boundary between oceanic dominated and continent dominated sediments is the most important feature of Figure 15. If one uses the factor dominance in surface sediments as an indicator of the present environment of deposition, then subsurface sediments, if they are displaced, are likely to have a different factor dominance than surface sediments from the same core. There are basically five possibilities to be considered (Table 1). They will be discussed below.

Factor Dominance in Subsurface Sediments

As shown in Figure 16, the dominant factor in the surface sediments is not necessarily the dominant factor in subsurface sediments. Cores 24, 25, 55, 56, 57, 58, 77, 78, and V35 have sediments at depth that are substantially different from the surface sediments from the same core. Cores 4, 5, 6, 7, 8, 12, 14, 17, 19, 21, 22, 59, 61, 70, 83, 130, 131, 134, and R76 have subsurface sediments similar to their surface sediments.

In order to account for a significant change in factor dominance in the sedimentary section it seems likely that there must have been a change in dispersal path, a tectonic juxaposition of sediment types, or

TABLE 1. Factor Dominance Situations

Surface Factor Dominance	Subsurface Factor Dominance	Physiographic Setting	Interpretation	Examples (cores)
1. oceanic	oceanic	Nazca Plate, Nazca Ridge	normal pelagic sedimentation	Y71-6-4P RC9-76 Y71-6-12P
2. oceanic	oceanic	Continental slope	continental accretion	Y71-6-24P HIG 130 HIG 131
3. oceanic	continental	Nazca Plate, continental slope	tectonism(a) or change in sedimentation pattern (b)	Y71-8-77P(a) V15-35(b) Y71-8-55F(b) 56F, 57F, 58F(b)
4. continental (A or B)	continental	Continental margin	normal hemi-pelagic sedimentation	Y71-6-5P Y71-6-6P
5. continental (A or B)	oceanic	Lower continental slope	continental accretion	Y71-6-25P

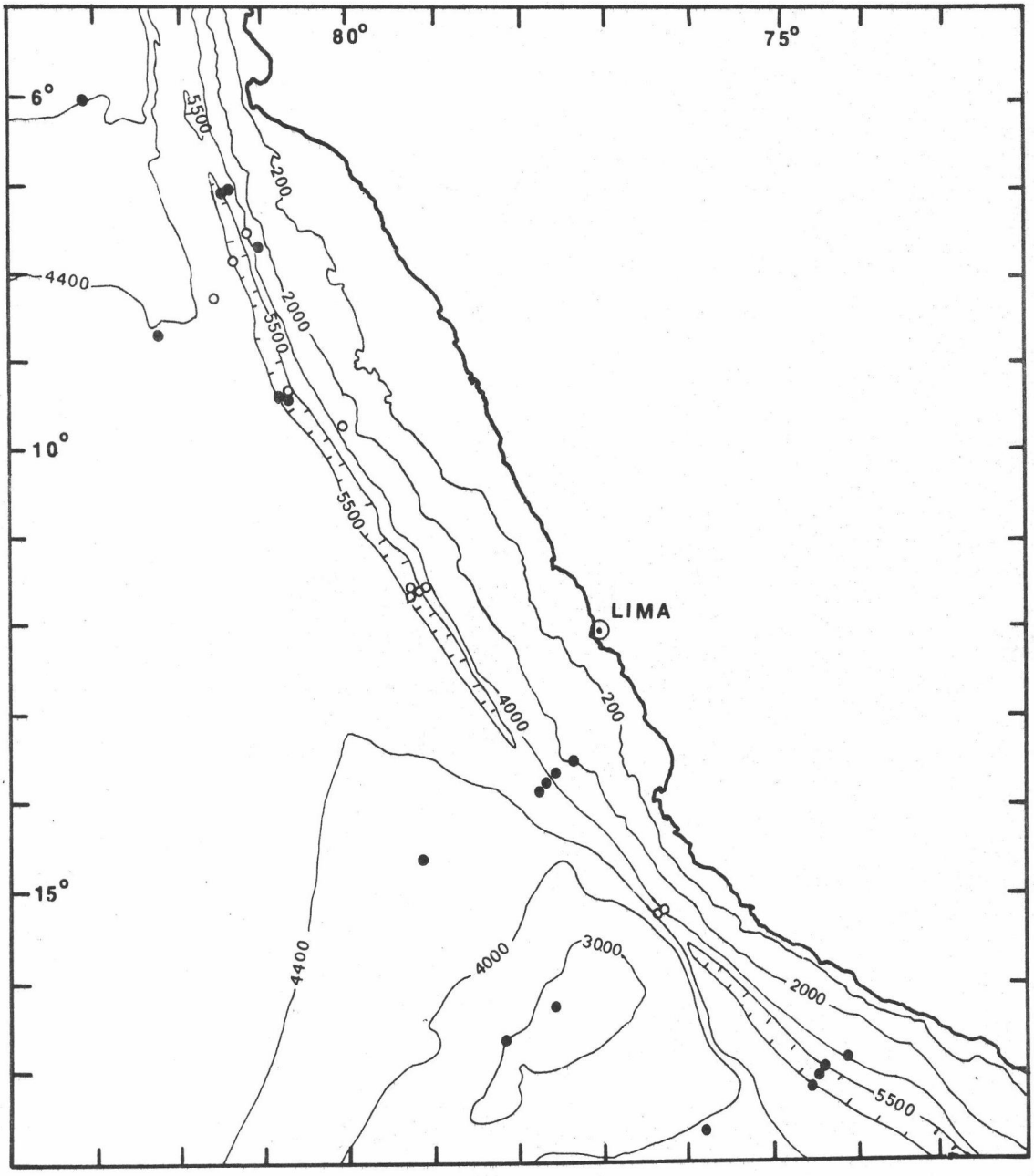

Figure 16. Comparison of surface and subsurface factor dominance. Open circles indicate that the surface and subsurface sediments are dominated by different factors. Solid circles indicate that there is no change in factor dominance with depth in a core.

a change in the source. Likewise, cores with uniform factor loadings indicate that there has not been a change in sediment input or tectonic mixing of the sediment.

The boundary between sediments with an oceanic dominance and those with a continental dominance shifted up to 100 km to the west of the present one during the Quaternary (Figure 15). In the case of cores 24, 74, 77, and 78 (Figure 16), this is due to deep water deposition of continental-type sediments by turbidity currents. In cores 55, 56, 57, 58, and V35, where samples were not taken from visibly graded turbidite intervals, there is some indication that normal hemipelagic sedimentation was dominated by continental assemblage A earlier in the Quaternary. This change occurred fairly recently; within the upper 6 cm of core 57 sediments change from oceanic dominance to continental dominance.

A seaward shift of the boundary between oceanic and continental sediments could have been caused by increased erosion rates and/or lowered sea level (which would cause a westward movement in the shoreline) during Pleistocene glacial stages. The greatest change in the distance between present and past positions of the factor dominance boundary coincides with the wider shelf from 8°30' to 12°S (Figure 15). Between 13° and 15°S there was little change in the position of the boundary, possibly because there may be higher sedimentation rates in this area and because sediments with high continental factor

loadings deposited seaward of the trench have been subducted. As one would suspect, this shift in the position of the boundary is accompanied by a slight increase in continental character (factor 2 loadings) between surface and basal sediments in some cores (59, 61, 65, and 78; Appendix II).

Some cores on the continental margin do not show a change from dominantly continental to oceanic influence (e.g., cores 83, 130, and 131), but are oceanic in character throughout; they probably represent accreted pelagic sediments. It is unlikely that continental margin sediments would not contain continental-type assemblages at depth because earlier in the Quaternary sediments dominated by the continental factor extended farther to the west. Non-deposition of continental assemblages on topographic highs, such as the knoll on the continental slope where core 83 was recovered, is possible, but not in the case of cores 130 and 131 at the base of the continental slope. Other cores (6, 24, and 25) probably indicate continental accretion has occurred, but since the interpretations are more complicated, they will be discussed along with other cores in the same seismic profile.

RELATION OF SEDIMENT DISTRIBUTION TO STRUCTURAL SETTING

In this chapter, I will examine the lithology of the sediments

recovered from the poorly defined structural features in the Peru Trench area, particularly the lowermost continental slope. The locations of the seismic profiles are shown in Figure 17.

Profile A

Seismic reflection profile A (Figure 18), the northernmost profile across the Peru continental margin, shows that cores 130 and 131 were taken on outcrops of acoustic basement or areas with few coherent internal reflections on the lower continental slope. Both of these cores are composed of gray-green lutite. Core 130 has essentially the same factor loadings from the top to the bottom, while core 131 shows a decrease in oceanic influence (factor 1 loadings) and an increase in continental influence (factor 2 loadings) with depth. Because nearby cores on the continental slope have sediments dominated by a continental assemblage (73 and 74), cores 130 and 131 may be oceanic sediments accreted from the west. Core 131 probably was originally deposited closer to the continent than core 130 because it shows more of a continental character with depth.

Profile B

Cores 72 and 73 contained sand-silt turbidites throughout (Figure 19). The surface sediment from core 73 is dominated by continental assemblage A. The general lithology of both cores is

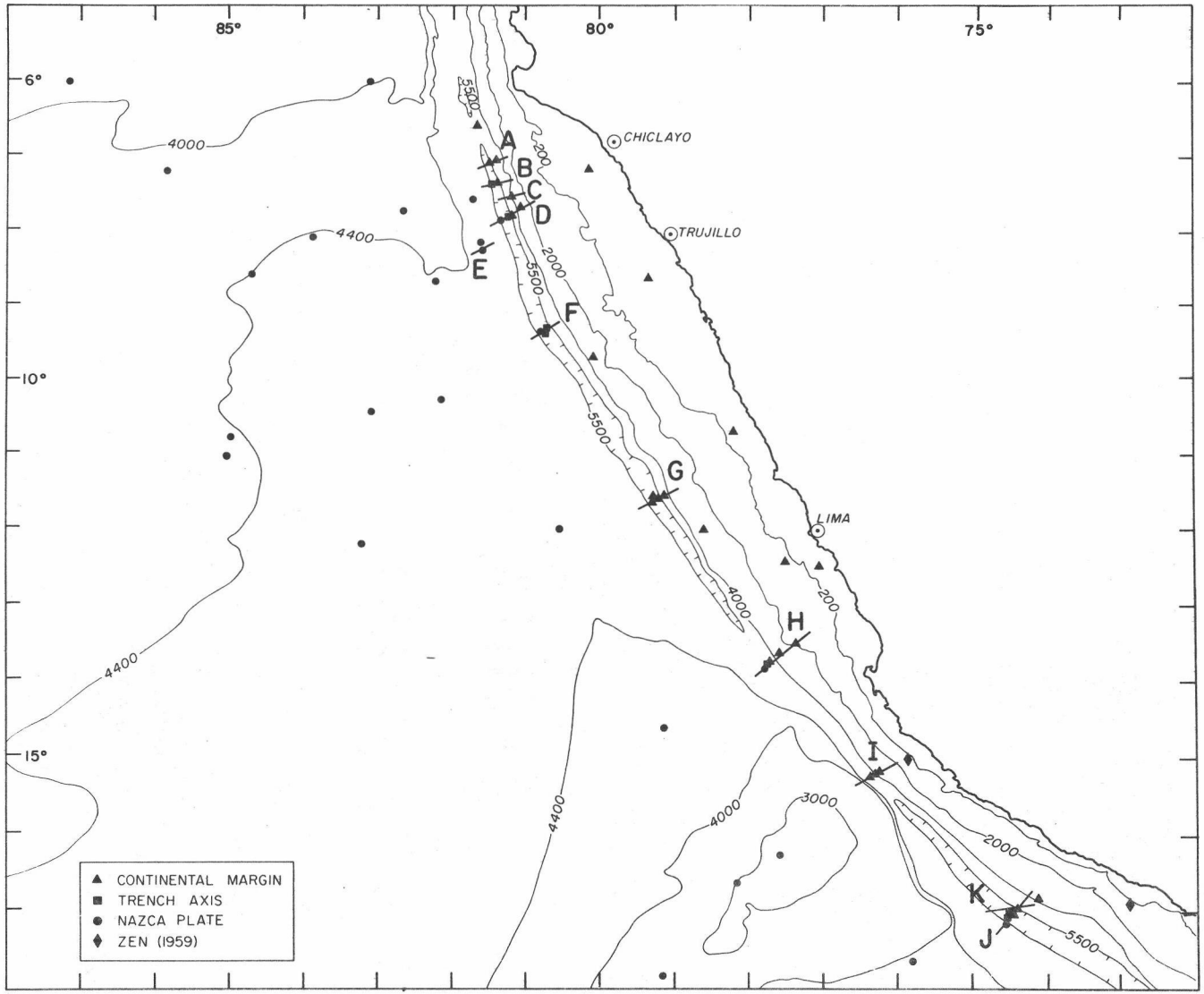

Figure 17. Location of seismic reflection profiles (A-K).

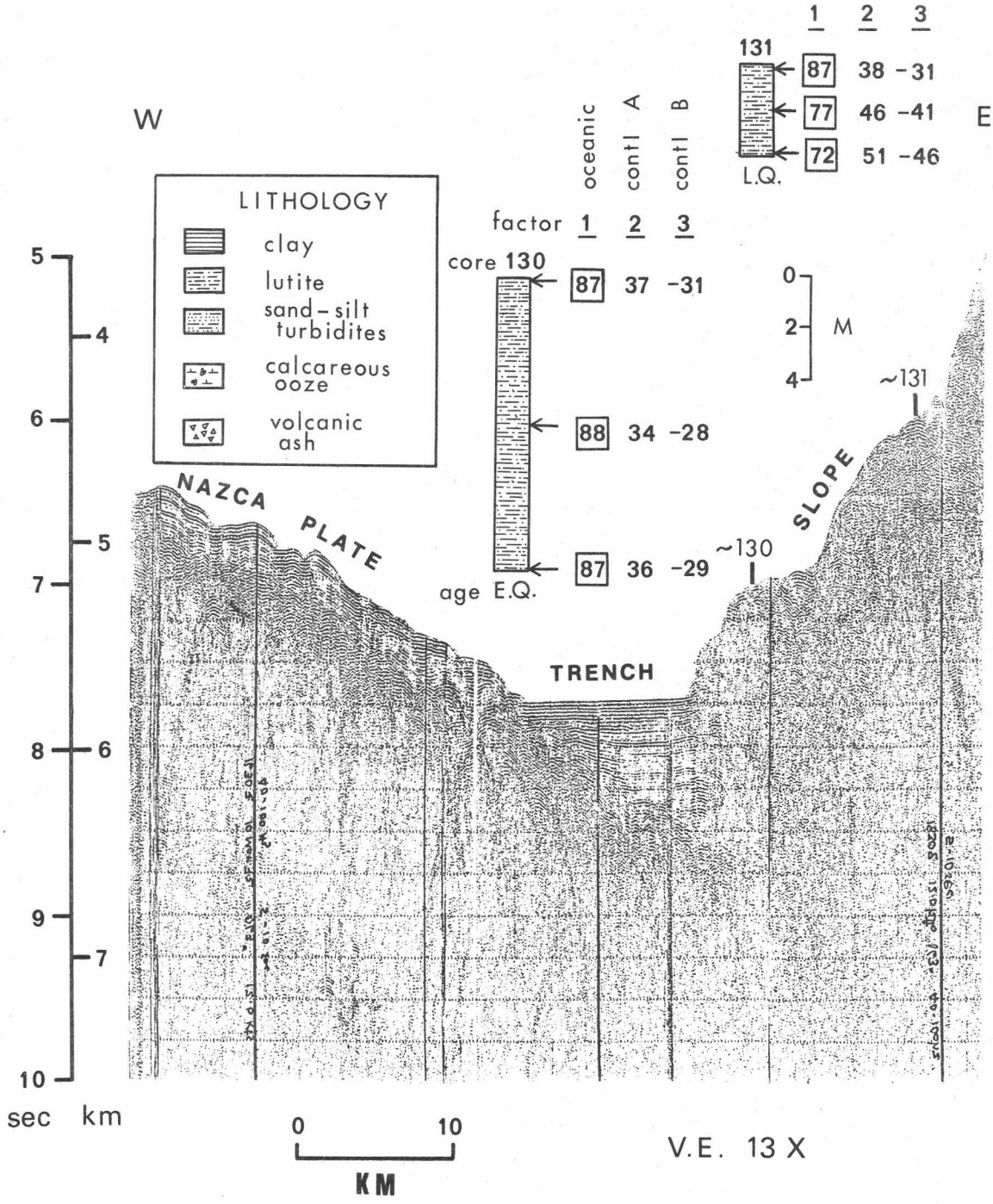

Figure 18. Seismic profile A. In this figure and in subsequent seismic profiles, the factor loadings have been multiplied by 100 and rounded to two figures. Boxes indicate the dominant factor for each sample. Radiolarian ages are given for the basal sample for each core. L. Q. = late Quaternary ($\leq$0. 4 m. y.); E. Q. = early Quaternary (between 0. 4 m. y. and 2. 0 m. y.).

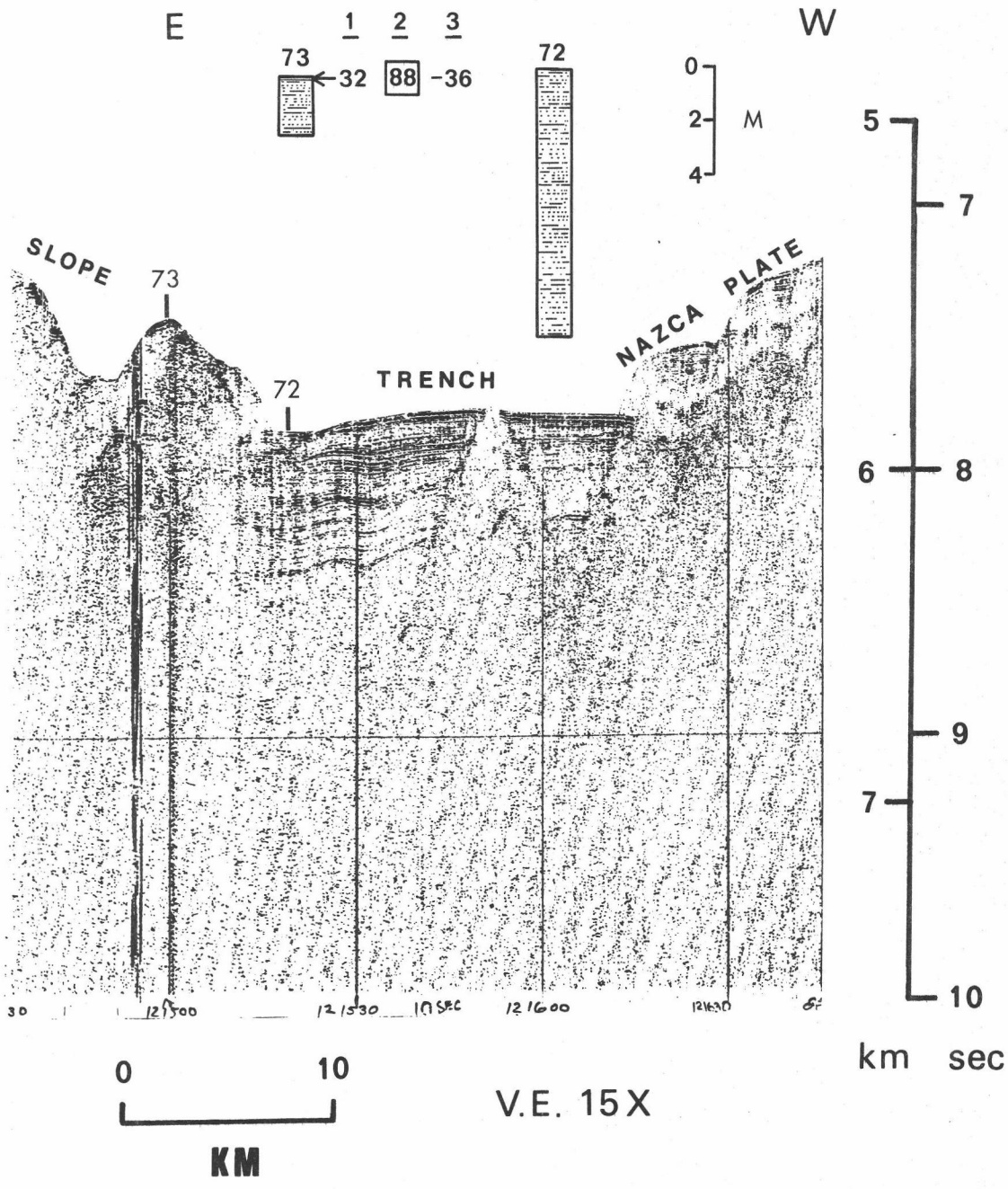

Figure 19. Seismic profile B. See Figure 18 for explanation. Core 73 is not uplifted 150-200 m above the surrounding topography; the portion of profile B to the left of core 73 is actually parallel to the continental slope. Note buried ridge in the trench axis and the landward-dipping trench sediments.

typical for the area.

Profile C

The steep scarp on the middle continental slope in profile C is comprised of turbidites except for the hemipelagic surface layer (core 74; Figure 20). The base of the core is continental-dominated sediment while the surface is oceanic. The lithology of the core is typical for this site. Like core 131, core 74 shows the effects of the seaward shift in the isopleths of continental factor loadings during the Pleistocene.

Profile D

Sand-silt turbidites are charcteristic of free-fall cores 80, 81, and 82, and core 79 contains olive gray lutite (Figure 21). Again, the sediments at the base of the continental slope lack coherent acoustic reflectors. Core 78 lies on the seaward wall of the Peru Trench, about 400 m above the trench floor, and contains pelagic sediments with an oceanic-dominated assemblage at the surface. The middle section of the core is composed of turbidites, implying an uplift of 400 m of the basin or previous trench axis relative to the present axis floor. The basal sediments of the core appear hemipelagic in character with no strong factor dominance, like sample 127-1 on the adjacent continental shelf. The relative uplift of this depositional

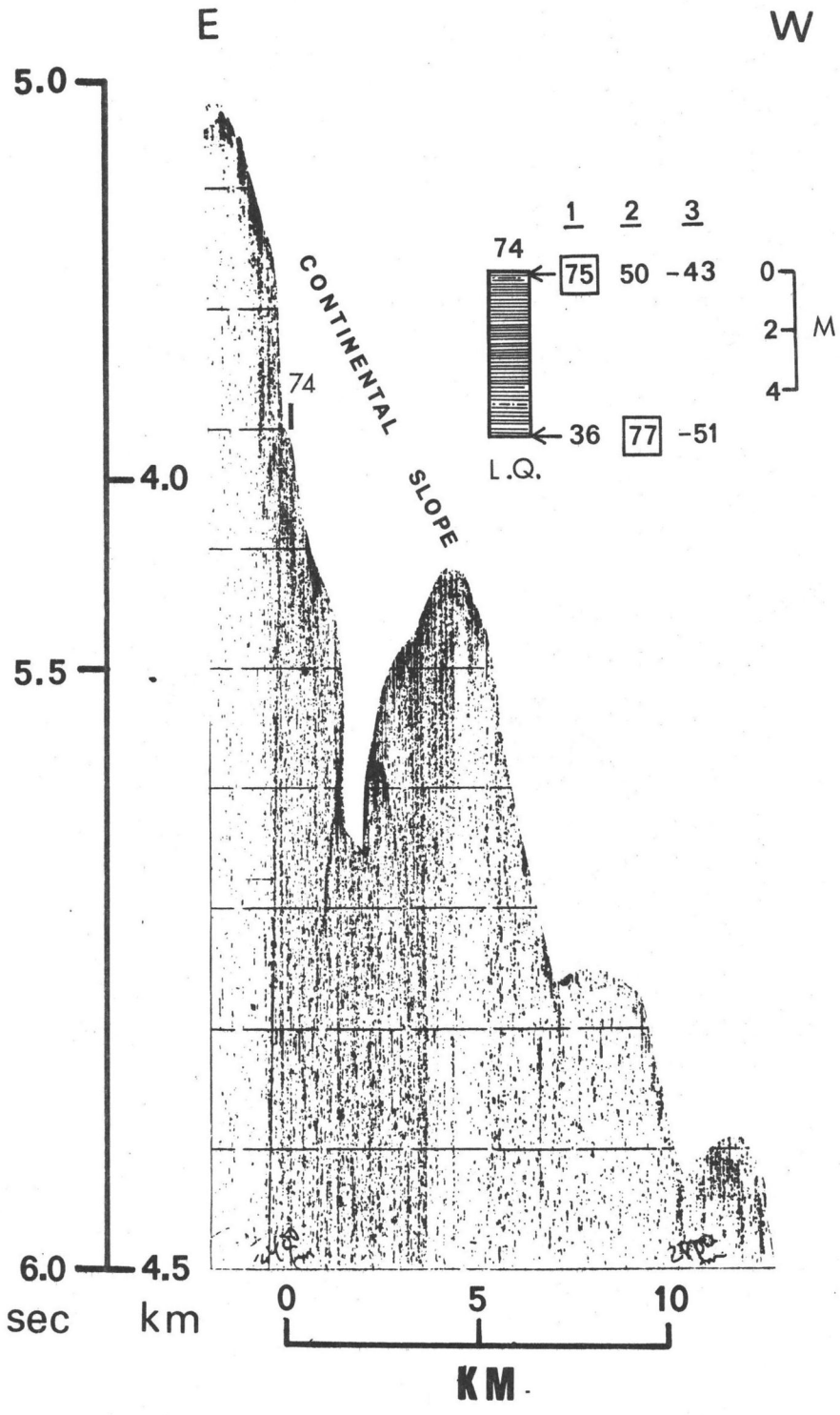

Figure 20. Profile C. See Figure 18 for explanation. This is a 3.5 kHz echogram; air gun records are not available for this station.

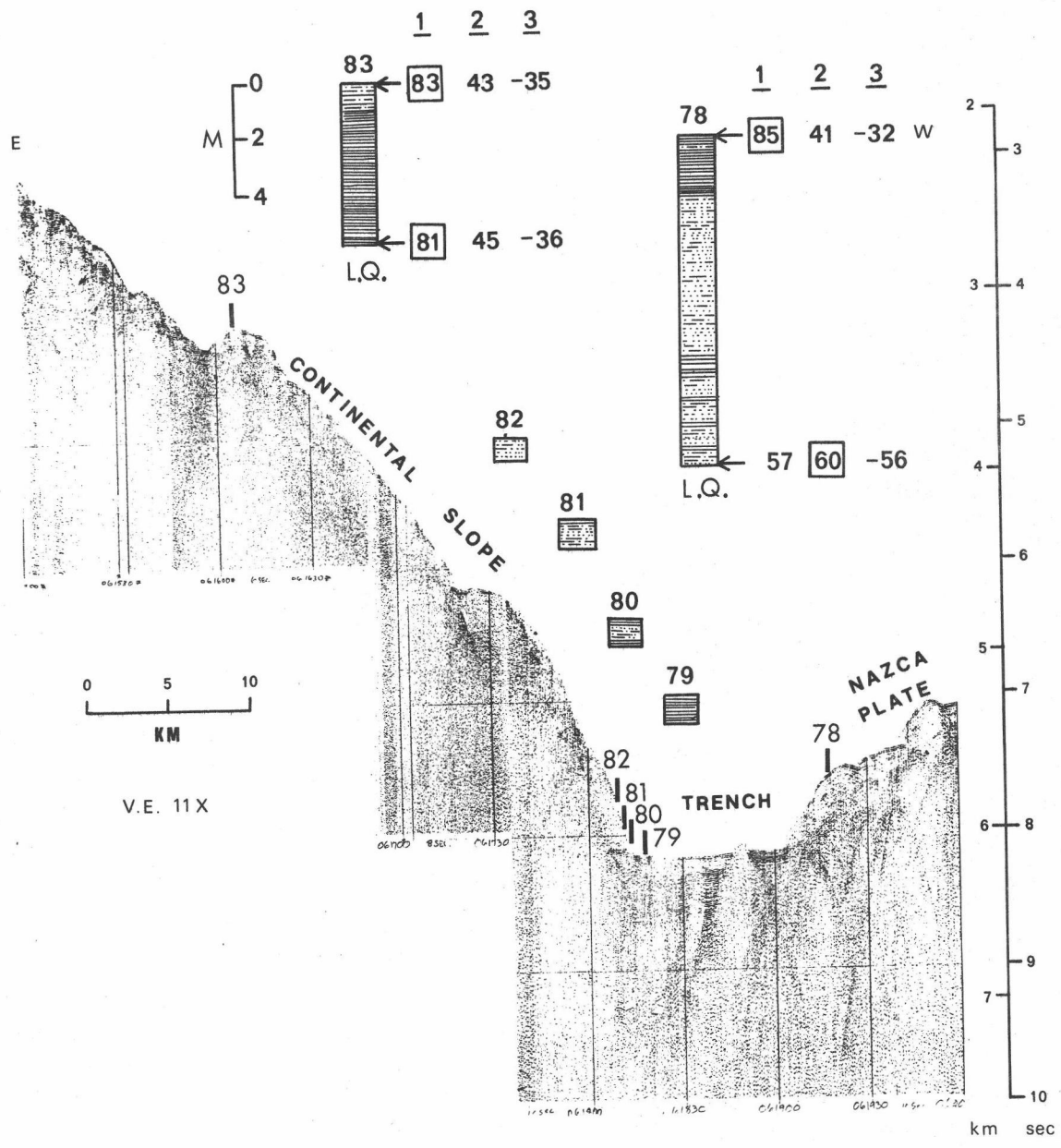

Figure 21. Seismic profile D. See Figure 18 for explanation.

site agrees with the sense of motion of another basin that contains terrigenous turbidites (cores 76 and 77) on the seaward side of the trench (Prince, 1974).

Core 83 was collected on a 150 m high knoll on the middle continental slope; it is composed of olive gray lutite and lacks turbidites. Like core 74, the surface sediment is dominated by an oceanic assemblage. However, unlike cores 74 and 78, which lie below and to the west of it, respectively, the basal sediments of this core are dominated by an oceanic assemblage. These deposits probably represent accreted oceanic sediments from the Nazca Plate.

Profile E

Prince (1974) described the uplifted turbidite basins about 50 km west of the present trench axis in which cores 76 and 77 were taken (Figure 22). A radiocarbon date of 5100 years b. p. (Prince and others, 1974) was obtained for the youngest turbidite. This gives a hemipelagic sedimentation rate of about 1.7 cm/1000 years. The base of the uppermost graded turbidite unit in core 77 has a factor 2 (continental assemblage A) dominance, while a hemipelagic interval just below it has a factor 1 (oceanic assemblage) dominance (Figure 22). The surface sediment from core 76 (Figure 22) also displays an oceanic dominance.

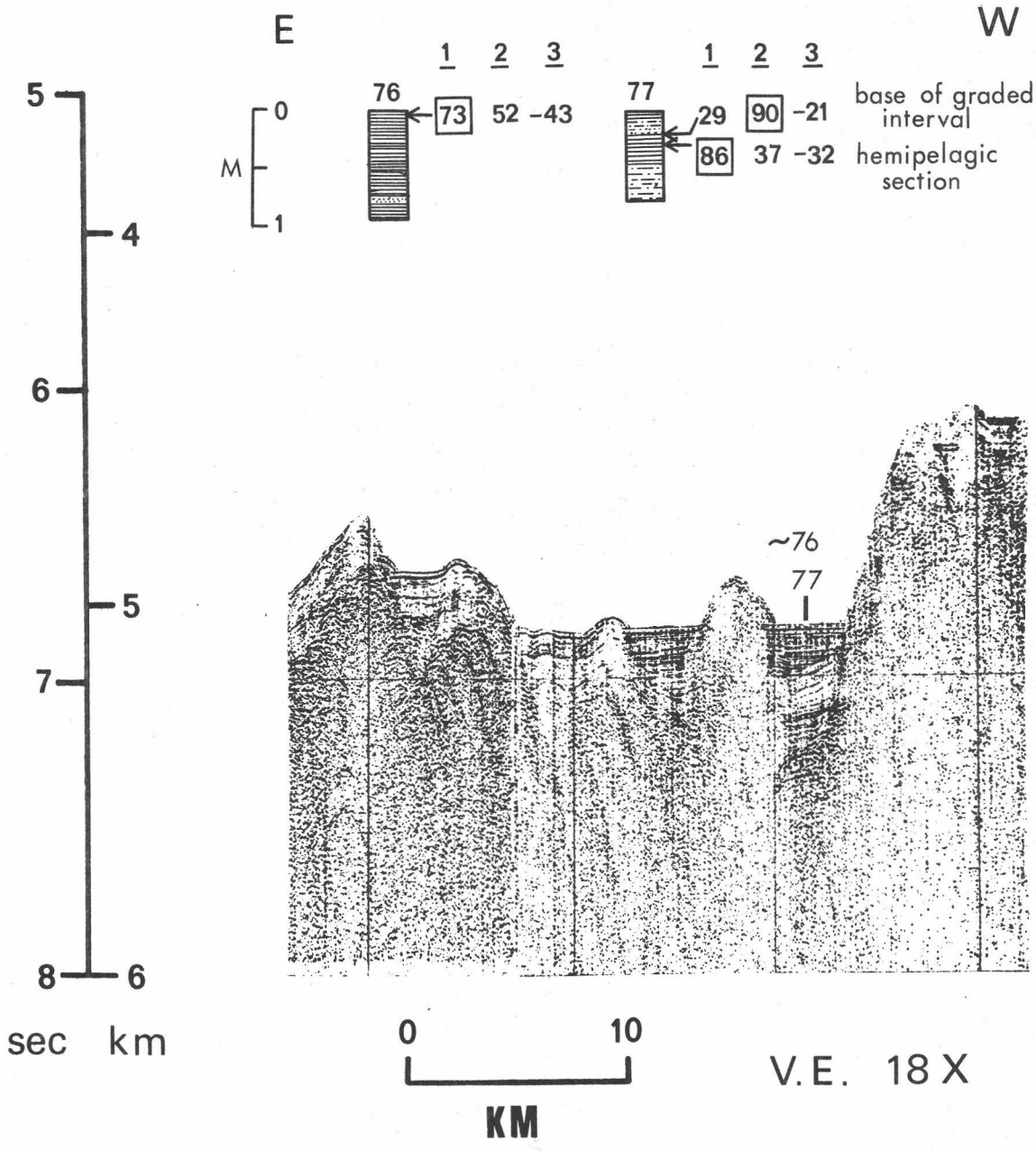

Figure 22. Seismic profile E. See Figure 18 for explanation.

Profile F

Two cores (59 and 65) were taken on a tholeiitic basalt ridge that rises about 900 m above the axis of the Peru Trench separating it into an inner deeper basin and an outer shallower basin (Kulm and others, 1973; Figure 23). They showed that the trench has been deformed within the past 400,000 yrs. Core 61 is located on the seaward wall of the trench. It contains turbidites and implies uplift on the seaward wall of the trench. The sediments from cores 59 and 65 near the top of the ridge have an oceanic dominance at the surface and at the bottom. The factor loadings at the base of each core are less oceanic than at the surface. This implies a westward shift in the isopleths of continental factor loadings. The turbidites in core 67 contain mixed-layer clays (Prince, unpublished research), a characteristic of factor 2 (continental assemblage A) dominated sediments.

Profile G

Several free-fall cores (55, 56, 57, and 58) were taken near the base of the continental slope at about 11°30'S (Figure 24). Sand and silt turbidites intercalcated with olive gray muds comprise cores 55 and 56. Cores 57 and 58 are olive gray lutites throughout. All four of the cores have surface sediments with an oceanic factor dominance and basal sediments with a continental factor A dominance. Plausible interpretations for this change in factor dominance from

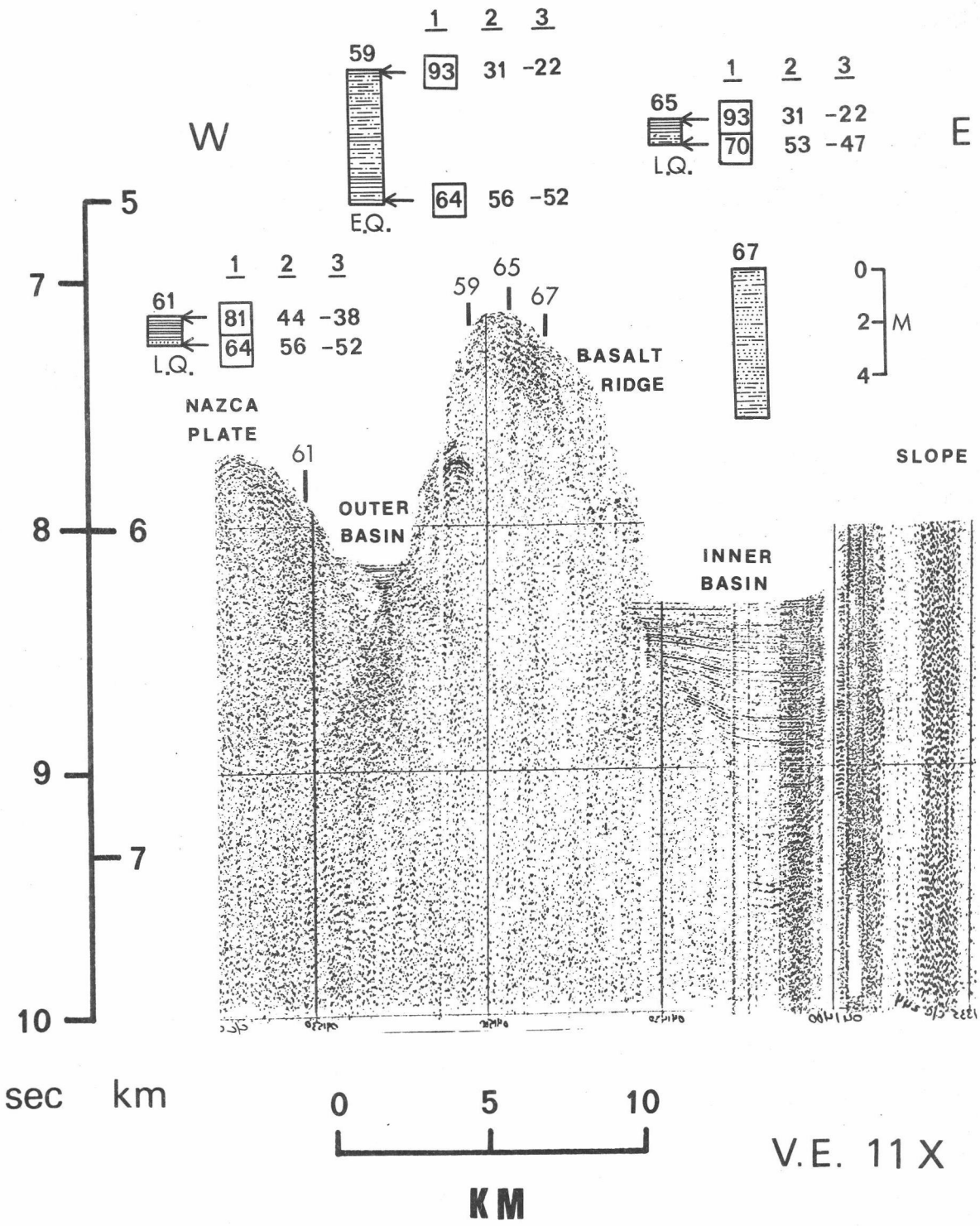

Figure 23. Seismic profile F. See Figure 18 for explanation. The reflection profile east of the inner basin is of very poor quality.

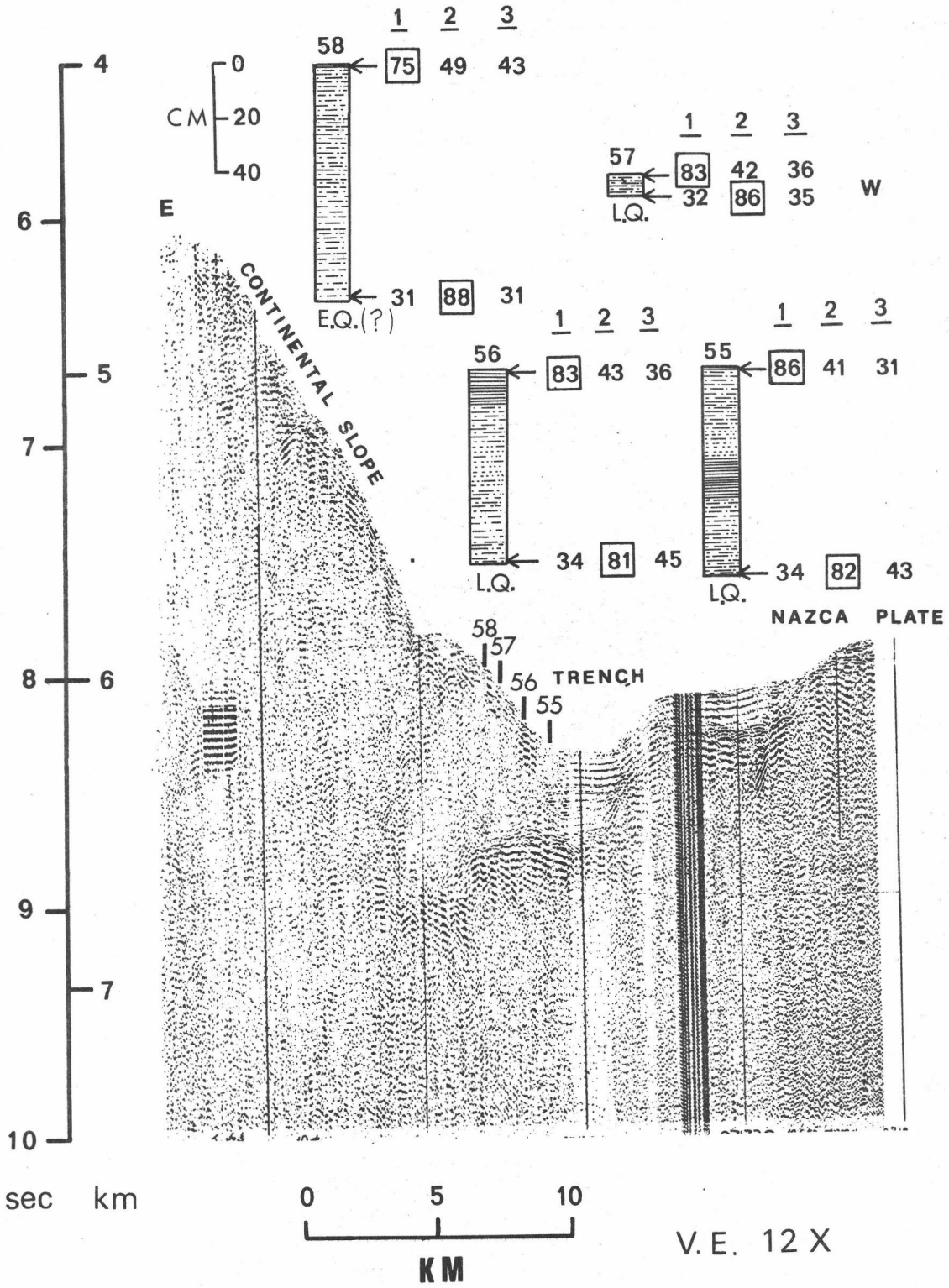

Figure 24. Seismic profile G. See Figure 18 for explanation.

continental to oceanic are: (1) continental sediments were transported downslope as turbidity currents, or (2) normal hemipelagic sediments at that site were formerly dominated by a continental assemblage, possibly during glacial ages when sea level was lowered and/or erosion rates were greater. The first interpretation is more feasible for cores 55 and 56; the second for 57 and 58. Part of the difficulty in analyzing cores 57 and 58 is the distinction between hemipelagic sediments and the tail of a turbidite.

Profile H

Seismic profile H is a traverse across the Peru Trench and continental margin southwest of Lima (Figure 25). Two free-fall cores along this profile contain turbidites (cores 9 and 10; Figure 25). Free-fall cores 8 and 11 contain hemipelagic lutites. Core 7, on the seaward side of the trench, was pelagic clay throughout. On the middle continental slope, core 6, except for a 2 cm thick layer of dolomite, was olive gray lutite.

Surface and basal sediments from cores 5, 6, and 8 on the landward side of the trench are primarily continental (factor 2 dominance). The surface and basal sediments of core 7 are dominantly oceanic. The only unusual feature in cores along this profile is the dolomite in core 6, which is probably diagenetically altered calcareous sediment.

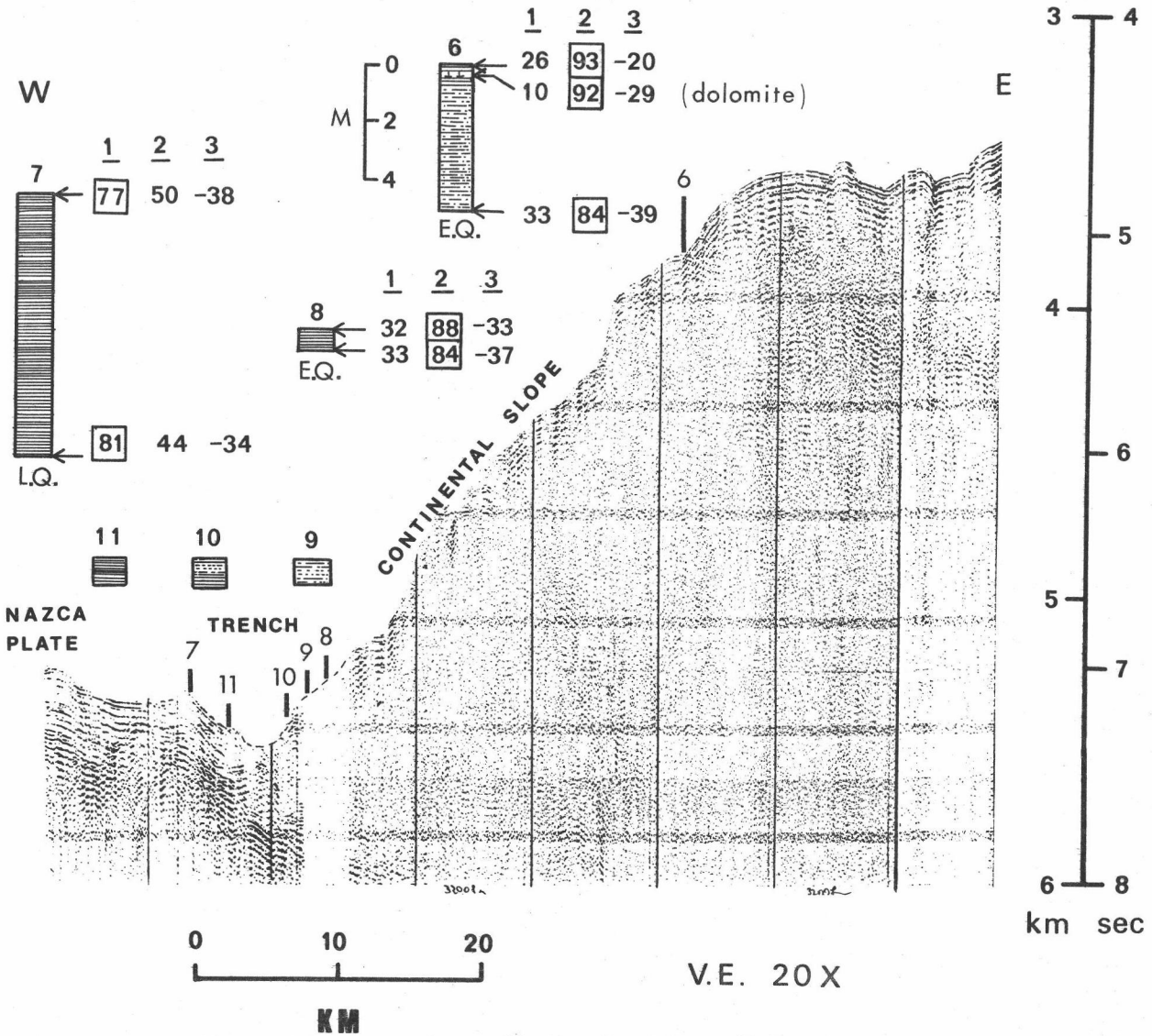

Figure 25. Seismic profile H. See Figure 18 for explanation.

The impure dolomite from core Y71-6-6P merits further discussion. Its clay mineralogy and organic carbon content are more like surface samples from landward of the trench than from seaward of the trench, yet its carbonate content is unusually high (49%) for samples from the continental margin. No calcareous microfossils were visible in scanning electron microphotographs of the rock. The carbonate-free fraction of the rock is composed chiefly of large diatoms (Coscinodiscus sp.), a few specimens of the Quaternary Radiolaria Plectacantha cremastoplegma Nigrini, and rare specimens of the post-middle Pliocene diatom Coscinodiscus africans (Burckle, 1972).

What is the origin of the rock? The presence of both dolomite and smectite-chlorite intergrades in the same rock indicates diagenetic alteration by Mg-rich solutions. (By comparison, the calcite in core Y71-6-12P was low magnesian calcite and there were no mixed-layer clays.) The presence of many large, relatively unbroken opaline components indicates a source near the coastal upwelling area. Sediments with both high carbonate content and a moderate organic carbon content (2.6%) generally occur on topographically high areas near a biologically productive area.

The impure dolomite might represent deeply buried pelagic sediments that originated on the fossil Galapagos Rise (Figure 1) that have been exposed during the process of continental accretion. If this

were true, the sediment should be very old, at least as old as anomaly 18 (basement age; Herron, 1972), and there would be very few diatoms in the material. This explanation does not seem plausible. If the rock were originally a foram-rich graded interval deposited in the trench-margin area, it should contain some admixed arkosic sand. It does not. The unique combination of sediment characteristics described above occurs only in sediments deposited on the Nazca Ridge.

How could the Nazca Ridge have been the source of the dolomite in core 6? Because the Nazca Ridge is apparently being subducted at an oblique angle to the trench (Isacks and others, 1968), a part of the Nazca Ridge may have been opposite the site of core Y71-6-6P. A convergence rate of 10 cm/yr is calculated for this area (Minster and others, 1974). About 3 m.y. ago, carbonate material slumped off the ridge in the manner similar to that described for the carbonate-rich sediments of the Nazca Ridge (core 24; Kulm and others, 1974). Subsequent uplift of the lower slope and diagenetic alteration of the calcite could give rise to the dolomite found in core 6.

Profile I

Figure 26 shows seismic reflection profile I across the margin, trench, and Nazca Ridge. The tectonic implications and general lithologies of cores 25 and 24 on the lower continental slope, and 12

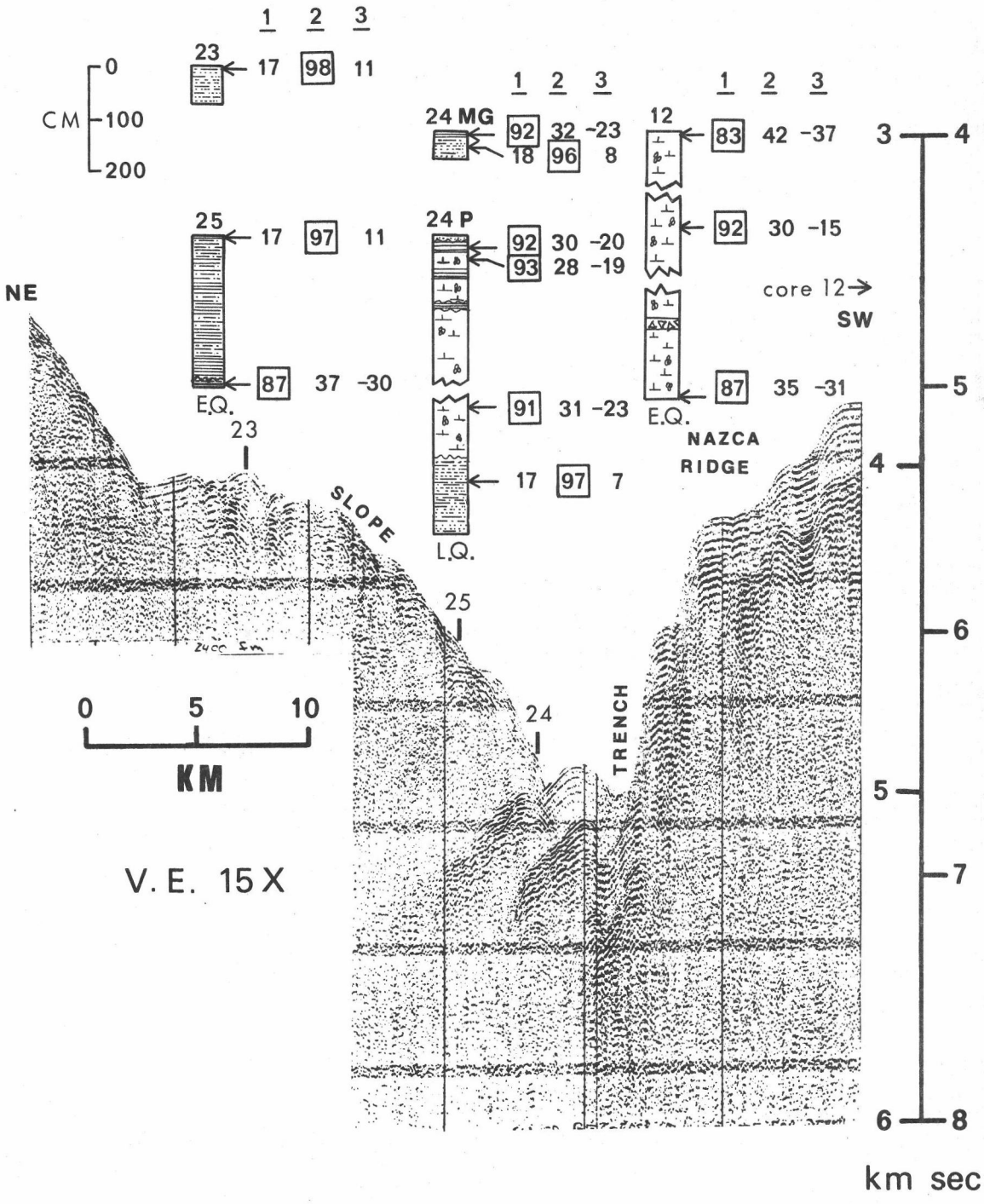

Figure 26. Seismic profile I. See Figure 18 for explanation. Core 12 was recovered on the Nazca Ridge about 200 km southwest of core 24.

on the Nazca Ridge have already been reported in Kulm and others (1974). They demonstrated that the carbonate-rich sections in core 24 came from the Nazca Ridge, the only source of foram-nannofossil ooze in the area. These deposits were folded against or thrust beneath the lower slope within the past 400,000 years. This study provides some additional information about the provenance of the carbonate-poor sections in core 24 and supports their conclusion on the origin of the carbonate-rich sections.

From the factor loadings of the surface sediments (Figures 15 and 26) it is clear that the boundary between oceanic dominated and continental dominated sediments lies between cores 24 and 25. Nowhere else on the Peru continental margin is this boundary as well defined. The oceanic character of the surface sediments in sample 24-1 is similar to other surface sediments from the lower slope (> 2000 m). The surface sediments in cores 23 and 25 have the same factor loadings as the turbidites from the gravity core (sample 24-2) and from the turbidites near the base of the piston core (sample 24-6).

The factor loadings in the carbonate-rich sections of core 24 are different from the factor loadings of calcareous ooze from the middle of core 12 on the Nazca Ridge (Figure 26) and from the surface sediments of cores R76 and R77 farther to the southwest on the Nazca Ridge. If the Nazca Plate and the South American Plate are converging, the Early Pliocene and Pleistocene carbonate oozes

in core 24 on the lower slope (Kulm and others, 1974) should have factor loadings similar to sediments now found at the surface at sites R76 and R77 and at depth in core 12. The subsurface sediments in cores 12 and R76, however, do not have monotonically increasing oceanic factor loadings with depth (Appendix III). As in core 4 (Figure 11), irregular fluctuations in factor loadings are difficult to interpret. The fluctuations may be due to changing dispersal patterns.

There are two remaining questions about the sediments in cores 24 and 25. Are the basal sediments in core 25 and the upper carbonate-poor clay sections in core 24 accreted pelagic sediment? The basal deposit in core 25 is distinctly different from the surface deposits from the same core. The boundary between the two types of sediment is near 286 cm. Hemipelagic olive gray (5Y3/2) lutites occur above this level, while homogeneous grayish olive (10Y4/2) clays occur below.

The oceanic factor dominated, greenish gray (5G6/1) carbonate-poor clay sections in core 24 (sample 24-3) contrast sharply with the intercalated carbonate-rich sections above and below it. Both the basal sediment from core 25 and the carbonate-poor clays in core 24 probably were originally deposited seaward of the present oceanic factor-continental factor dominance boundary and below the calcite compensation depth. Because the carbonate-poor clay in core 24 lacks much silt and sand size material and because it is Pliocene in

age (Kulm and others, 1974), it most likely originated seaward of the Peru Trench, probably on the northeastern slope of the Nazca Ridge. There are two possible interpretations of the basal sediments in core 25: (1) sediments dominated by the oceanic factor were deposited at this site during the early Quaternary until there was an influx of continental factor dominated sediments, or (2) the basal sediments are accreted oceanic sediment from the west. From the down-core information in other cores on the continental margin, the first interpretation is not feasible. Because the boundary between oceanic and continental factor dominated sediments shifted westward earlier in the Quaternary, basal sediments in cores on the continental margin should be more continental with depth. Therefore, the sediments at the base of core 25 appear to be accreted.

Profiles J and K

Profile J crosses the Peru Trench at 18°S (Figures 17 and 27), and profile K (Figure 28) intersects profile J. Turbidites were found on the lower continental slope (cores 15, 16, and 21) and in the trench (core 18). Core 20 on the seaward wall of the trench contains typical pelagic clays. Hemipelagic sediments and plant fragments comprised core 17. Factor loadings for all the cores (17, 19, 21, and 22) in this area indicate an oceanic influence for the sediments.

Using the criteria in Table 1, cores 17, 21, and 22 represent

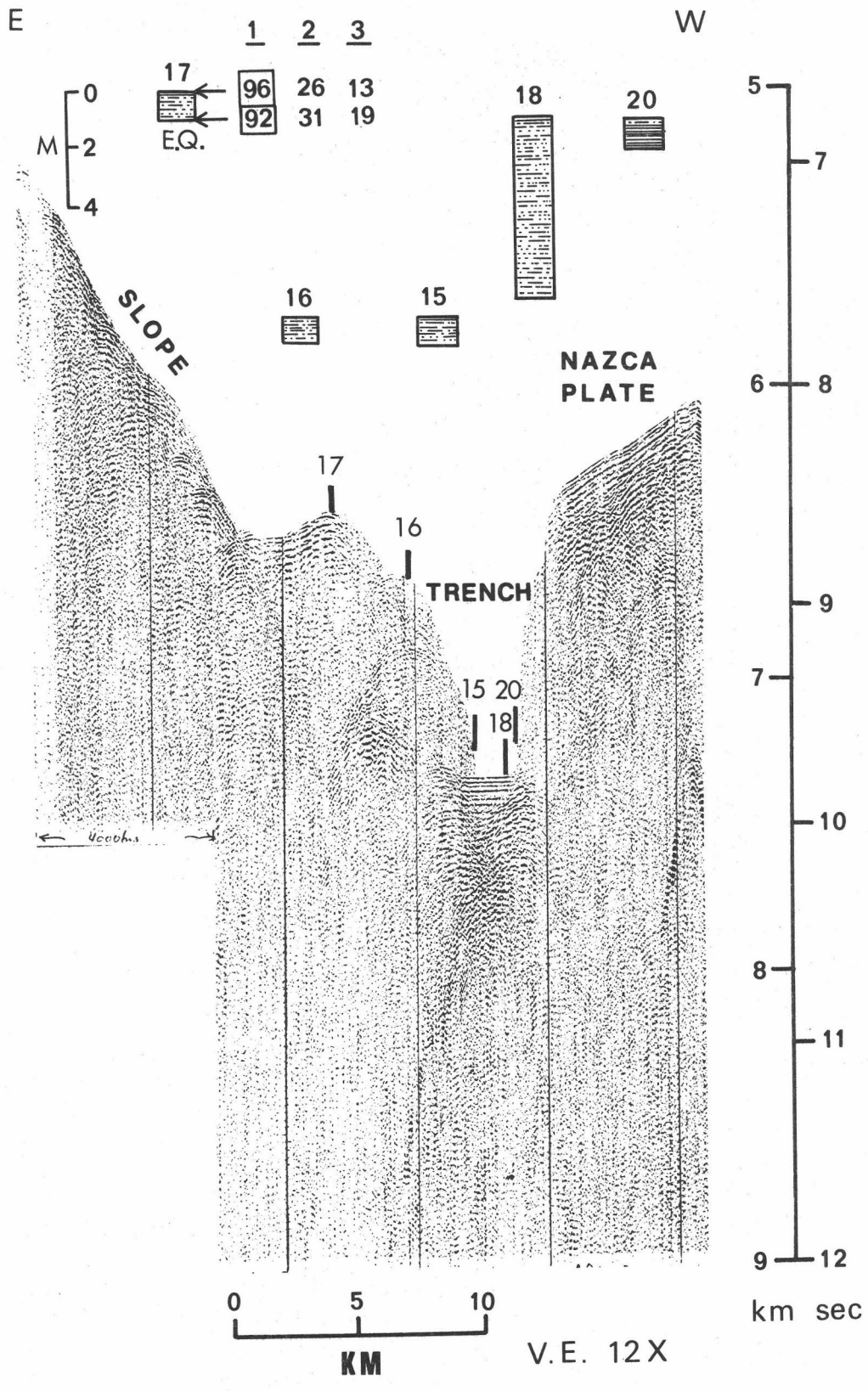

Figure 27. Seismic profile J. See Figure 18 for explanation. No seismic records are available for core 22.

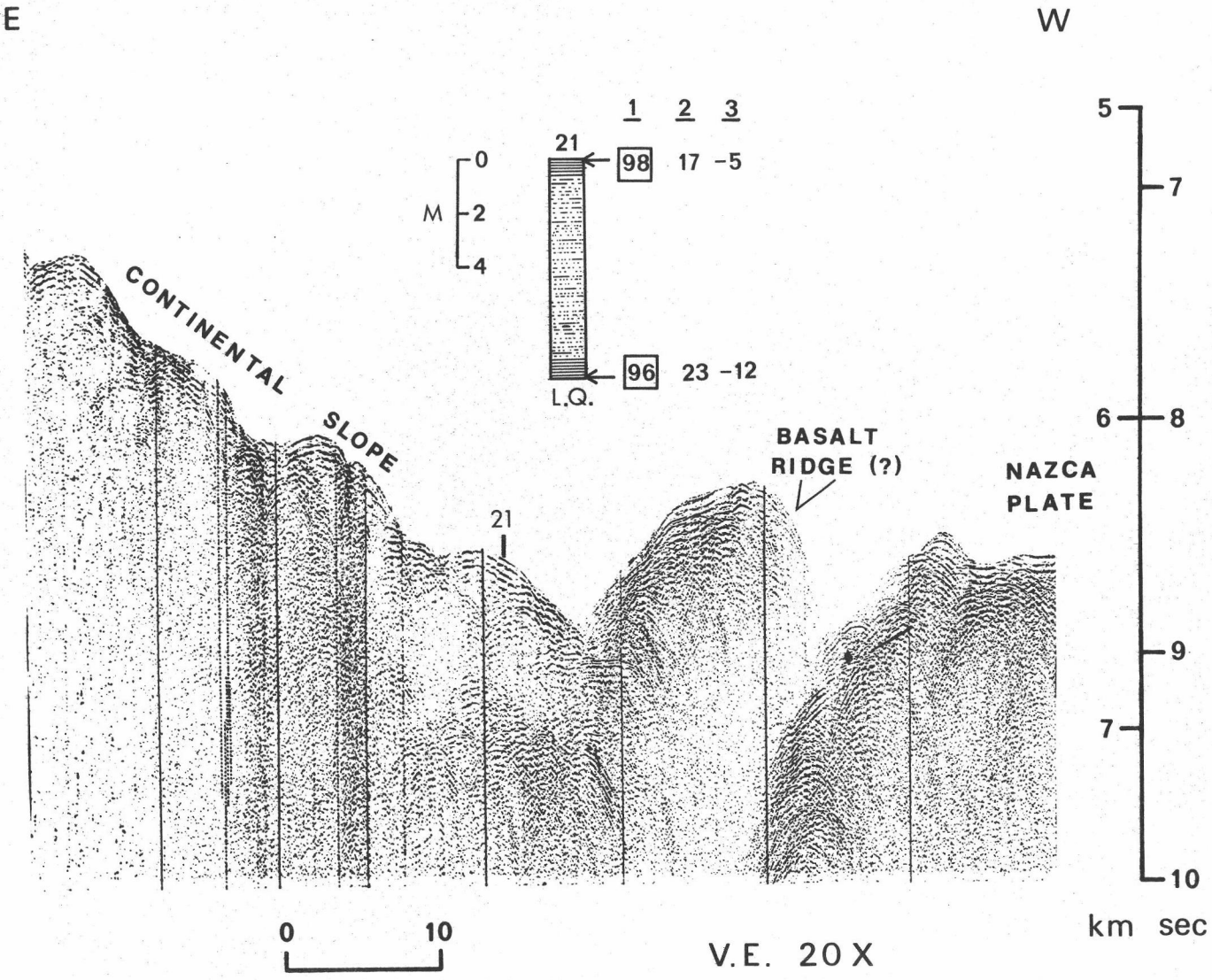

Figure 28. Seismic profile K. See Figure 18 for explanation.

accreted sediments. However, the uncertainties involved in fixing the oceanic factor-continental factor dominance boundary at this latitude, and the distinctive terrigenous overprint (plant fragments, graded turbidites) in these cores casts some doubt on the interpretation of continental accretion. Any sediments deposited to the west of core 22, whether they are found in the trench, the lower continental slope, or on the Nazca Plate could have an oceanic factor dominance. The question could be resolved by more detailed sampling both within the cores and on the sea floor in this region.

GENERAL DISCUSSION

From the surface distribution of clay minerals and organic carbon (Figures 4 to 8) and Q-mode factor analysis (Figures 12 to 16), the sediments off Peru have been fairly well characterized. Nazca Plate sediments are dominated by an oceanic assemblage composed mainly of smectite and aeolian illite. Upper continental margin sediments are dominated by continental-type assemblages comprised of mixed-layer smectite-chlorite, illite, kaolinite and chlorite, or illite, chlorite and kaolinite (Figure 10). Lower continental margin sediments are dominated by either an oceanic assemblage or continental assemblage A, which reflects the present abundance of smectite and illite in hemipelagic sediments and the downslope movement of continental-factor dominated sediments, respectively.

What can be said about the nature of the lowermost continental slope off Peru? Sixteen of the 28 cores taken on the acoustically complex landward wall of the trench contain sand-silt turbidites and hemipelagites of continental origin. Six cores contain sediments that appear to be oceanic sediments accreted from the Nazca Plate (Figure 29).

The best documented example of continental accretion is core 24, which consists of typical continental margin sediments that are interspersed with typical deep-sea pelagic sediments. Figure 26 shows the general lithology of core 24 as well as other cores in the same profile across the continental slope, trench and Nazca Ridge. Surface sediments at site 24 are oceanic in character, which is neither unusual for surface sediments on the lower continental slope (Figure 15) nor indicative of continental accretion (Table 1). What is unique about this core is that oceanic factor dominated sediments are found between continental factor dominated turbidite sections. The main problem in interpreting the factor loadings for these deposits is that the hemipelagic surface sediments (sample 24-1), the carbonate-poor clays (sample 24-3), and the calcareous ooze sections (samples 24-4 and 24-5) all have similar factor loadings. We know from biostratigraphic evidence that the carbonate-rich sections of the core came from the Nazca Ridge (Kulm and others, 1973). The carbonate-poor clay sections (sample 24-3) must also be

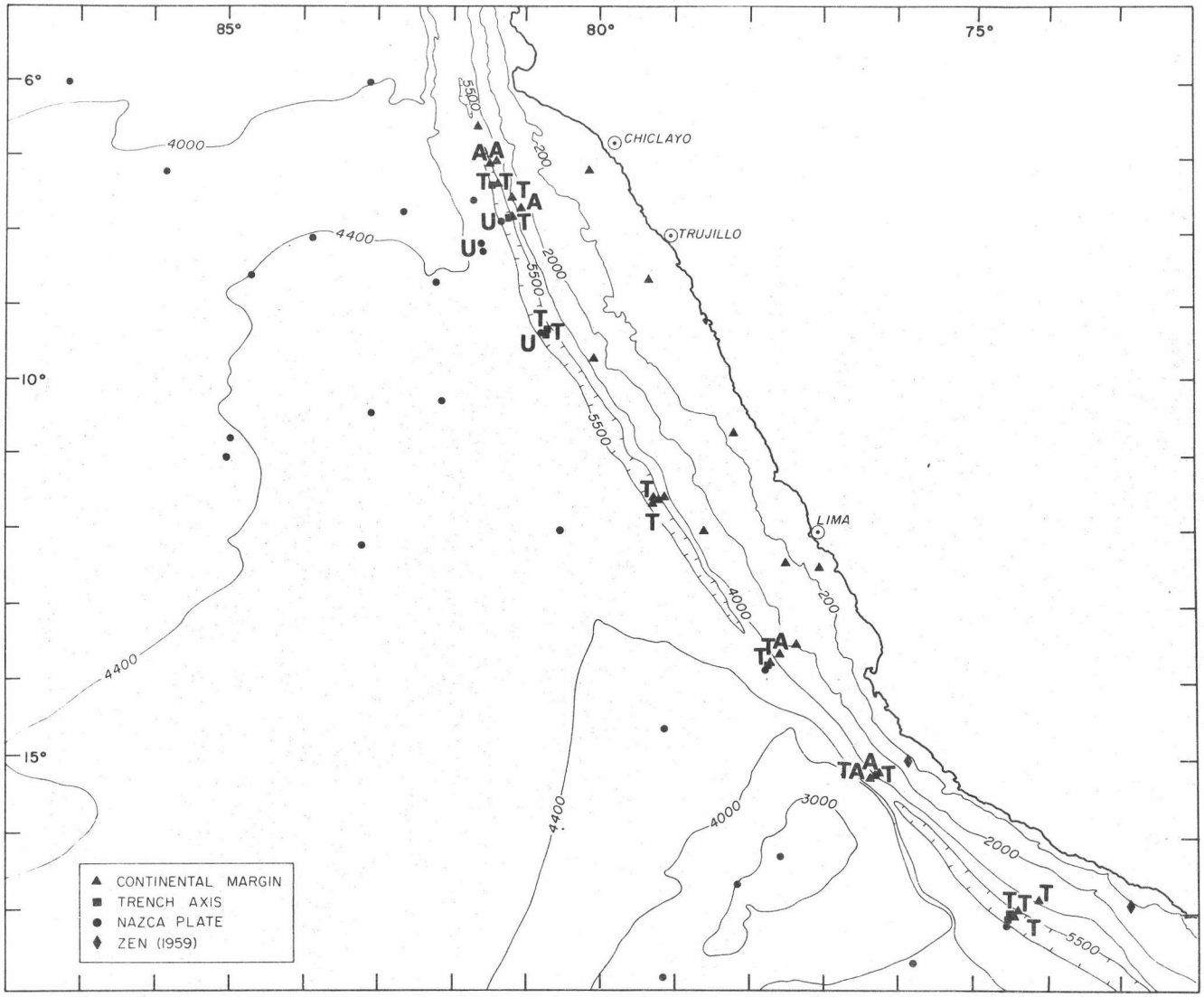

Figure 29. Types of sediments in the trench-margin area. T = turbidites; A = accreted oceanic sediments; U = uplifted turbidites seaward of the present trench axis.

accreted sediments because they are Pliocene in age. If the carbonate-poor sections were originally deposited at site 24, then they should be either hemipelagites or terrigenous turbidites of late Quaternary age. The fine grain size (> 50% clay) of the carbonate-poor clay suggests that the clay was deposited seaward of the trench.

The oceanic factor dominated sediments at the base of core 25 are early Quaternary in age ($0.4 \leq X < 2.0$ m.y.). Late Quaternary (≤ 0.4 m.y.) continental factor dominated sediments were recovered near the base of core 24 (sample 24-6). Thus, the late Quaternary factor dominance boundary was west of core 24 but the early Quaternary boundary may have been east of core 25. If this is the case, the basal sediments of core 25 are not displaced and do not represent accreted sediments. One would expect, however, that the factor dominance boundary in the early Quaternary to extend farther seaward than core 24 because erosion rates now are probably their lowest. Moreover, a lowering of sea level during a glacial stage would tend to move the boundary seaward.

The impure Quaternary dolomite recovered on the lower continental slope (core 6) is probably calcareous sediment originally deposited on the Nazca Ridge that has been transferred to the continental margin. Its mineralogy (dolomite and mixed-layer smectite-chlorite) and position (over 1800 m above the present trench axis) suggest diagenetic alteration by Mg-rich solutions and uplift of the

lower continental slope. The dolomite could not be deeply buried pelagic sediments that originated on the fossil Galapagos Rise because it is too young (post middle Pliocene) and because it contains too many diatoms. Neither could the sediments have been a foram-rich turbidite derived from the continental margin because foram-rich graded intervals on the Peru margin always contain some admixed detrital sand and they are much lower in carbonate percentage (e.g., samples 77-1, 0.84% $CaCO_3$; 24-2, 1.42% $CaCO_3$).

The most likely source of diatom-rich, high carbonate sediments with moderate organic carbon content is the Nazca Ridge. This implies left-lateral displacement of the Nazca Ridge along the axis of the Peru Trench, slumping of calcareous Nazca Ridge sediments into the trench, and subsequent uplift of the lower continental slope. The transfer of Nazca Ridge sediments to the Peruvian continental margin has been documented elsewhere (core 24, Kulm and others, 1974). The calcareous sediments in core 24, however, are not altered to dolomite.

Cores 83, 130, and 131 also indicate continental accretion. Even after the effect of a seaward shift in the factor dominance boundary is taken into account (Figure 15), the subsurface sediments in these cores appear to be displaced. The oceanic factor loading and the lack of turbidites in subsurface sediments suggests an original deposition site seaward of the trench. In order for deep-sea

pelagic sediments to occur on the middle continental slope there must have been a tremendous amount of uplift. Core 83 is located about 3000 m above the present trench axis and is younger than 0.4 m.y. A reasonable alternative explanation is that the knoll on which core 83 is located has been a topographic high for the last 0.4 m.y. Consequently, bottom seeking currents with a continental factor dominance by-passed the area.

Core 130 (early Quaternary) and core 131 (late Quaternary), because they lie at the base of the slope, are expected to have some terrigenous overprint. Since they do not, cores 130 and 131 are apparently Nazca Plate sediments that have been piled against or thrust beneath the lower continental slope, and subsequently uplifted to their present position.

In summary, there are six cores (6, 24, 25, 83, 130, and 131) on the middle to lower continental slope off Peru that have sediments which probably originated on the Nazca Plate. These cores range from about 300 m (24) to about 3000 m (83) above the present trench axis. Sediments in two of these cores (samples 6-2, 24-4, and 24-5), because of their distinctive carbonate and micropaleontological components, probably originated on the Nazca Ridge. One core (83) on the middle continental slope because of its young age ($\leq$0.4 m.y.) and its topographic setting, may be either accreted Nazca Plate sediments or sediments that have accumulated out of the influence of

continental factor dominated sediments. Cores 25, 130, and 131 because of their low carbonate contents and their lack of definitive microfossils, make full use of the Q-mode factor analysis technique to demonstrate continental accretion.

CONCLUSIONS

With the aid of Q-mode factor analysis, three factors (oceanic, continental A, and continental B) can explain 99% of the variation in clay mineral composition and organic carbon content in surface sediments off Peru. The oceanic factor accounts for 65% of the variance and represents sediments dominated by smectite and subordinate illite. Continental factor A accounts for 25% of the variance and represents sediments composed of mixed-layer clays, illite, chlorite, and kaolinite. The third factor, continental factor B, accounts for 10% of the variance and represents sediments dominated by illite with subordinate chlorite and kaolinite.

The boundary between surface sediments with an oceanic factor dominance (i.e., factor loadings for the oceanic factor in a sample are higher than the continental factor loadings) and surface sediments with a continental factor (A or B) dominance lies on the continental slope. Earlier in the Quaternary, this boundary was seaward of its present position because turbidity currents deposited continental factor dominated sediments on the seaward side of the present trench

axis (cores 61, 76, 77, and 78). In addition, nearshore hemipelagic sediments were more continental in character during the early Quaternary, possibly because of increased erosion rates and a seaward shift of the shoreline during glacial stages. The presence of the turbidites on the seaward side of the trench between 7°30' and 9°30'S demonstrates relative uplift in these areas (Figure 29).

Accreted oceanic sediments on the continental slope can be recognized by comparing the surface factor dominance with the subsurface factor dominance and by noting the position of the factor dominance boundary. Where subsurface oceanic sediments are landward of this boundary (as in cores 24 and 25 at the base of the continental slope, and core 83 on the middle continental slope), accretion from the Nazca Plate is suggested. The oceanic dominated sediments in cores 130 and 131, because they were recovered from the base of the continental slope and because nearby cores are distinctly terrigenous (72 and 73), also are accreted Nazca Plate sediments. One core (6) is over 1800 m above the trench floor and contains dolomite that probably was formed from calcareous ooze originally deposited on the Nazca Ridge. It was transferred to the Peruvian continental margin by some mechanism associated with subduction (e.g., slumping and imbricate thrusting) and diagenetically altered to dolomite. In order for the Nazca Ridge to have been the source of the carbonate, there may have been left-lateral displacement of the Nazca Ridge along the

Peru Trench.

Accreted pelagic sediments, however, are by no means the major constituent of the near-surface sediments on the landward wall of the Peru Trench. This region is characterized by a distinct terrigenous overprint of sand-silt turbidites and hemipelagic lutites. Perhaps accreted oceanic sediments will be found beneath the continentally derived sediments in this area when deeper holes are drilled into the lower continental slope.

BIBLIOGRAPHY

Berggren, W. A. (1972) A Cenozoic time scale - some implications for regional geology and paleobiogeography. Letheia. 5:195-215.

Besoain, E. (1969) Clay mineralogy of volcanic ash soils. In: Inter-American Institute of Agricultural Science, O.A.S., Panel on Volcanic Ash Soils in Latin America, July 6-13, 1969, Turrialba, Costa Rica. B.1.1 - B.1.16.

Biscaye, P. E. (1965) Mineralogy and sedimentation of recent deep-sea clay in the Atlantic Ocean and adjacent seas and oceans. Geol. Soc. America Bull. 76:803-832.

Brown, G. W., Ed. (1962) The X-ray identification and crystal structures of clay minerals. Jarrold and Sons, Ltd. London. 544 p.

Burckle, L. H. (1972) Late Cenozoic planktonic diatom zones from the Eastern Equatorial Pacific. In: Simonsen, R., ed., Proc. first symposium on Recent and fossil marine diatoms. Bremerhaven, Sept. 21-26, 1970. 39:217-245.

Carstea, D. D. (1965) Conditions of Al, Fe, and Mg interlayer formation in montmorillonite and vermiculite. M.S. thesis. Corvallis, Oregon State University. 73 numb. leaves.

_____ (1967) Formation and stability of Al, Fe, and Mg interlayers in montmorillonite and vermiculite. Ph.D. thesis. Corvallis, Oregon State University. 117 numb. leaves.

Chave, K. E. (1952) A solid-solution between calcite and dolomite. Jour. Geol. 60:190-192.

Chichester, F. W., Youngberg, C. T. and M. E. Harward (1969) Clay mineralogy of soils formed on Mazama pumice. Soil Soc. America Proc. 33:115-120.

Cobbing, E. J. and Pitcher, W. S. (1972) Plate tectonics and the Peruvian Andes. Nature. 240:51-53.

Dinkelman, M. G. (1973) Radiolarian stratigraphy: Leg 16, Deep Sea Drilling Project. In: van Andel, T. H., Heath, G. R. et al. (eds.), Initial Reports of the Deep Sea Drilling Project, Vol. 16, Washington (U. S. Government Printing Office), p. 747-813.

_____ (1974) Late Quaternary Radiolarian paleo-oceanography of the Panama Basin, Eastern Equatorial Pacific. Ph. D. thesis. Corvallis, Oregon State University. 123 numb. leaves.

Dixon, J. B. and Jackson, M. L. (1962) Properties of intergradient chlorite-expansible layer silicates of soils. Soil Sci. Soc. America Proc. 26:358-362.

Donoso, L. (1959) Clay fraction of some soils of Chile. Societe Francaise de Mineralogies et de Cristallographie Bull. 82:361 363.

Eklund, W. A. (1974) A microprobe study of metalliferous sediment components. M. S. thesis. Corvallis, Oregon State University. 77 numb. leaves.

Grim, R. E. (1968) Clay mineralogy, 2nd ed. McGraw-Hill Book Co. New York. 596 p.

Gross, M. G., Carey, A. G., Jr., Fowler, G. A., and Kulm, L. D. (1972) Distribution of organic carbon in surface sediments, northeast Pacific Ocean. In: Pruter, A. T. and Alverson, D. L., eds., The Columbia River estuary and adjacent ocean waters. University of Washington Press, Seattle, p. 254-264.

Griffin, J. J., Windom, H. and Goldberg, E. D. (1968) The distribution of clay minerals in the world ocean. Deep-Sea Res. 15:433-459.

Harward, M. E., Theisen, A. A., and Evans, D. D. (1962) Effect of iron removal and dispersion methods on clay mineral identification by X-ray diffraction. Soil Sci. America Proc. 26:533-541.

Hays, J. D. (1970) Stratigraphy and evolutionary trends of Radiolaria in North Pacific deep-sea sediments. In: Hays, J. D., ed., Geological Investigations of the North Pacific. Geol. Soc. America Mem. 126:185-218.

Hayes, J. B. (1973) Clay petrology of mudstones, Leg 18, Deep Sea Drilling Project. In: Kulm, L. D., von Huene, R., et al., 1973, Initial Reports of the Deep Sea Drilling Project, Vol. 18, Washington (U. S. Government Printing Office), p. 903-914.

Heath, G. R., Moore, T. C., Jr., and Roberts, G. L. (1974) Mineralogy of surface sediments from the Panama Basin, Eastern Equatorial Pacific. Jour. Geol. (in press).

Herron, E. M. (1972) Sea floor spreading and the Cenozoic history of the east-central Pacific. Geol. Soc. America Bull. 83:1671-1692.

Ingle, J. C., Jr. and Karig, D. E. (1973) Leg 31, Western Pacific floor. Geotimes. 18:22-25.

Imbrie, J. and Kipp, N. G. (1971) A new micropaleontological method for quantitative paleo-climatology: Application to a late Pleistocene Caribbean core. In: Turekian, K. K., ed., The late Cenozoic glacial ages. Yale University Press, New York. p. 71-181.

Imbrie, J. and van Andel, Tj. H. (1964) Vector analysis of heavy mineral data. Geol. Soc. America Bull. 75:1131-1156.

Isacks, B., Oliver, J. and Sykes, L. R. (1968) Seismology and the new global tectonics. Jour. Geophys. Res. 77:5855-5899.

Jackson, M. L. (1963) Interlayering of expansible layer silicates in soils by chemical weathering. Clays and Clay Min. 11:29-46.

Kendrick, J. (1974) Trace element studies of metalliferous sediments in cores from the East Pacific Rise and Bauer Deep, 10°S. M.S. thesis. Corvallis, Oregon State University. 117 numb. leaves.

Klovan, J. E. and Imbrie, J. (1971) An algorithm and Fortran-IV program for large scale Q-mode factor analyses and calculation of factor scores. Math. Geol. 3:61-77.

Kulm, L. D., Scheidegger, K. F., Prince, R. A., Dymond, J., Moore, T. C., Jr., Hussong, D. M. (1973) Tholeiitic basalt ridge in the Peru Trench. Geology 1:11-14.

Kulm, L. D., Resig, J. M., Moore, T. C., Jr. and Rosato, V. J. (1974) Transfer of Nazca Ridge sediments to the Peru continental margin. Geol. Soc. America Bull. (in press).

Lisitzin, A. P. (1972) Sedimentation in the world ocean. Soc. Econ. Paleon. and Mineral. Spec. Publ. 17, 218 p.

Ludwig, W. J., Ewing, J. F., Ewing, M., Muranchi, M., Den, N., Asano, S., Hotla H., Hayakawa, M., Asanuma, T., Ichikawa, K. and Noyuchic, I. (1966) Sediments and structure of the Japan Trench. Jour. Geophys. Res. 71:2121-2137.

Ludwig, W. J., Hayes, D. E., and Ewing, J. I. (1967) The Manila Trench and West Luzon Trough, 1, Bathymetry and sediment distribution. Deep-Sea Res. 14:533-544.

Malahoff, A. (1970) Some possible mechanisms for gravity and thrust faults under ocean trenches. Jour. Geophys. Res. 75:1992-2001.

McGinnes, W., Goldman, B. and Paylore, P. (1968) Deserts of the world, an appraisal of research into their physical and biological environments. University of Arizona Press. Tucson. 788 p.

McManus, D. A., Hanson, L. G., and Baker, J. V. (1966) A sample splitter for moist saturated, or suspended sediment. Jour. Sedimentary Petrol. 36:632-635.

Minster, J. B., Jordan, T. H., Molnar, P. and Haines, E. (1973) Numerical modeling of instantaneous plate tectonics. Geophys. Jour. Royal Astr. Soc. (in press).

Mehra, O. P. and Jackson, M. L. (1960) Iron oxide removal from soils and clays by a dithionite-citrate system buffered with sodium bicarbonate. In: Swineford, A., ed., Clays and Clay Minerals, Proc. 7th Natl. Conf., Pergamon Press, London. p. 317-327.

Nigrini, C. A. (1968) Radiolaria from eastern tropical Pacific sediments. Micropaleontology. 14:51-63.

Oinuma, K., Kobayashi, K. and Sudo, T. (1959) Clay mineral composition of some recent marine sediments. Jour. Sedimentary Petrol. 29:56-63.

Oxburgh, E. R. and Turcotte, D. L. (1971) Origin of paired metamorphic belts and crustal dilation in island arc regions. Jour. Geophys. Res. 76:1315-1327.

Powers, M. C. (1957) Adjustment of land-derived clays to the marine environment. Jour. Sedimentary Petrol. 27:355-372.

Prince, R. A. (1974) Deformation in the Peru Trench, 6° to 10°S. M. S. thesis. Corvallis, Oregon State University. 91 numb. leaves.

Prince, R. A., Resig, J. M., Kulm, L. D., and Moore, T. C., Jr. (1974) Recent vertical movements on the seaward edge of the Peru-Chile Trench (unpublished research).

Rex, R. W. (1967) Authigenic silicates formed from basaltic glass by more than 60 million years' contact with sea water, Sylvania Guyot, Marshall Islands. Clays and Clay Min. 15:195-203.

Rich, C. I. (1968) Hydroxy interlayers in expansible layer silicates. Clays and Clay Min. 16:15-30.

Rosato, V. J., Kulm, L. D., and Derks, P. S. (1974) Surface sediments of the Nazca Plate. Pacific Science (submitted).

Ross, D. A., and Shor, G. G., Jr. (1965) Reflection profiles across the middle America Trench. Jour. Geophys. Res. 70:551.

Sachs, H. M. (1973) Quantitative Radiolarian-based paleo-oceanography in late Pleistocene subarctic Pacific sediments. Ph. D. thesis. Providence, Brown University. 208 p.

Sawhney, B. L. (1958) Aluminum interlayers in soil clay minerals, montmorillonite and vermiculite. Nature. 182:1595-1596.

Scholl, D., von Huene, R. and Ridlow, J. (1968) Spreading of the ocean floor - undeformed sediments of the Peru-Chile Trench. Science. 159:869-871.

Scholl, D., Christensen, M., von Huene, R. and Marlow, M. (1970) Peru-Chile Trench sediments and sea floor spreading. Geol. Soc. America Bull. 81:1339-1360.

Seely, D. R., Vail, P. R., and Walton, G. G. (1974) Fore-arc structuring between the volcanic arc and trench. In: Burk, C. A. and Drake, C. L., (eds.) Continental Margins (in preparation).

Seyfert, C. K. (1969) Undeformed sediments in oceanic trenches with sea floor spreading. Nature. 222:70-72.

Smith, R. L., Enfield, D. B., Hopkins, T. S., and Pillsbury, R. D. (1971) The circulation in an upwelling eco-system: the Pisco cruise. Investigacion Pesquera. 35:9-24.

Stephan, I. and MacEwan, D. M. C. (1951) Some chlorite clay minerals of unusual type. Clay Minerals Bull. 1:157-162.

Suzuki, H. (1971) Climatic zones of the Wurm glacial age. Bull., Dept. Geogr. Univ. Tokyo. 3:35-46.

Trask, P. D. (1939) Organic content of recent marine sediments. In: Trask, P. D., ed., Recent marine sediments. Dover Publ., New York, p. 428-453.

von Huene, R. (1972) Structure of the continental margin and tectonism at the eastern Aleutian Trench. Geol. Soc. America Bull. 83:3613-3626.

von Huene, R. and Kulm, L. D. (1973) Tectonic summary of Leg 18. In: Kulm, L. D., von Huene, R., et al., 1973, Initial Reports of the Deep Sea Drilling Project, Vol. 18, Washington (U. S. Government Printing Office), p. 961-976.

von Huene, R. and Shor, G. G., Jr. (1969) The structure and tectonic history of the eastern Aleutian Trench. Geol. Soc. America Bull. 80:1889-1902.

Weaver, C. E. (1956) The distribution and identification of mixed-layer clays in sedimentary rocks. Amer. Mineral. 41:202-221.

Zen, E. (1959) Mineralogy and petrology of marine bottom sediment samples off the coast of Peru and Chile. Jour. Sedimentary Petrol. 29:513-539.

APPENDICES

APPENDIX I. Sample Identification

Core No.	Sample No.	Core Identification	Sample Interval (cm)	Core Length (cm)	Latitude °S	Longitude °W	Water Depth (m)	
3	3-1	Y71-6-3SS	0-1	N. R.	12°28.2'	77°02.7'	130	
4	4-1	Y71-6-4MG3	2.5-3.5	89	14°36.0'	79°05.5'	4423	
"	4-2	Y71-6-4P	66-67	1678	14°36.6'	79°07.2'	4518	
"	4-3	"	236-237	"	"	"	"	
"	4-4	"	406-407	"	"	"	"	
"	4-5	"	576-577	"	"	"	"	
"	4-6	"	746-747	"	"	"	"	
"	4-7	"	916-917	"	"	"	"	
"	4-8	"	1086-1087	"	"	"	"	
"	4-9	"	1256-1257	"	"	"	"	
"	4-10	"	1426-1427	"	"	"	"	
"	4-11	"	1596-1597	"	"	"	"	
"	4-12	"	1671-1672	"	"	"	"	A. L.
5	5-1	Y71-6-5MG1	0-1	N. R.	13°30.2'	77°19.9'	2286	
"	5-2	Y71-6-5P	230-231	463	"	"	"	
"	5-3	"	460-461	"	"	"	"	
6	6-1	Y71-6-6P	7-8	524	13°37.0'	77°34.2'	3801	
"	6-2	"	30-32	"	"	"	"	D.
"	6-3	"	522-523	"	"	"	"	
7	7-1	Y71-6-7MG3	3-5	68	13°45.7'	77°45.9'	5374	
"	7-2	Y71-6-7P	950-951	953	"	"	"	
8	8-1	Y71-6-8FF4	1-2	74	13°45.1'	77°42.8'	5273	
"	8-2	Y71-6-8FF4	71-72	"	"	"	"	
9		Y71-6-9FF3		75	13°45.4'	77°43.2'	5371	

APPENDIX I. Continued

Core No.	Sample No.	Core Identification	Sample Interval (cm)	Core Length (cm)	Latitude °S	Longitude °W	Water Depth (m)	
10		Y71-6-10FF2		83	13°45.7'	77°43.7'	5508	
11		Y71-6-11FF1		75	13°46.2'	77°44.4'	5594	
12	12-1	Y71-6-12MG3	7-8	100	16°26.6'	77°33.8'	2734	
"	12-2	Y71-6-12P	528-529	1260	"	"	"	
"	12-3	"	1256-1257	"	"	"	"	
"	12-4	"	1093-1094	"	"	"	"	A. L.
14	14-1	Y71-6-14MG3	2-3	80	17°40.2'	75°47.3'	4625	
"	14-2	Y71-6-14P	831-832	1600	"	"	"	
"	14-3	"	1594-1595	"	"	"	"	
15		Y71-6-15FF1		78	16°55.5'	74°21.8'	7406	
16		Y71-6-16FF3		72	16°54.5'	74°20.7'	6761	
17	17-1	Y71-6-17FF4	0-1	86	16°53.3'	74°20.0'	6485	
"	17-2	"	84-85	"	"	"	"	
18		Y71-6-18P		609	16°56.7'	74°21.3'	7280	
19	19-1	Y71-6-19MG3	2-4	64	17°03.0'	74°24.5'	5791	
"	19-2	Y71-6-19P	961-962	963	"	"	"	
20		Y71-6-20FF1		74	16°57.9'	74°20.8'	7293	
21	21-1	Y71-6-21MG2	3-4	60	16°50.8'	74°21.7'	6505	
"	21-2	Y71-6-21P	911.5-912.5	914	"	"	"	
22	22-1	Y71-6-22MG4	2-4	62	16°48.6'	74°03.4'	5301	
"	22-2	Y71-6-22P	345-346	690	"	"	"	
"	22-3	"	688-689	690	"	"	"	
23	23-1	Y71-6-23MG1	3-4	68	15°11.9'	76°14.7'	3920	
24	24-1	Y71-6-24MG1	3-4	44	15°16.0'	76°18.8'	4899	

APPENDIX I. Continued

Core No.	Sample No.	Core Identification	Sample Interval (cm)	Core Length (cm)	Latitude °S	Longitude °W	Water Depth (m)
24	24-2	Y71-6-24MG1	37-38	44	15°16.0'	76°18.8'	4899
"	24-3	Y71-6-24P	23-24	698	"	"	"
"	24-4	"	43-44	"	"	"	"
"	24-5	"	450-452	"	"	"	"
"	24-6	"	591.5-592.5	"	"	"	"
25	25-1	Y71-6-25P	5.5-6.5	294	15°15.5'	76°18.9'	4614
"	25-2	"	292-293	"	"	"	"
27	27-1	Y71-7-27MG1	4-5	87	10°14.6'	82°05.2'	4569
28	28-1	Y71-7-28MG1	8-9	74	11°01.0'	85°00.7'	4491
55	55-1	Y71-8-55FF1	3-4	78	11°38.5'	79°14.8'	6307
"	55-2	"	76-77	"	"	"	"
56	56-1	Y71-8-56FF2	3-4	72	11°38.4'	79°14.7'	6256
"	56-2	"	71-72	"	"	"	"
57	57-1	Y71-8-57FF4	0-1	7	11°38.0'	79°14.4'	6176
"	57-2	"	6-7	"	"	"	"
58	58-1	Y71-8-58FF5	4-5	86	11°37.6'	79°14.2'	6189
"	58-2	"	85-86	"	"	"	"
59	59-1	Y71-8-59MG5	4-5	73	9°21.8'	80°41.1'	5304
"	59-2	Y71-8-59P	495-496	514	"	"	"
61	61-1	Y71-8-61FF5	1-2	92	9°21.0'	80°46.9'	5843
"	61-2	"	90-91	"	"	"	"
65	65-1	Y71-8-65FF3	3-4	92	9°20.6'	80°41.1'	5468
"	65-2	"	90-91	"	"	"	"
67		Y71-8-67P		547	9°21.0'	80°41.1'	5603

APPENDIX I. Continued

Core No.	Sample No.	Core Identification	Sample Interval (cm)	Core Length (cm)	Latitude °S	Longitude °W	Water Depth (m)	
68	68-1	Y71-8-68G	0-1	N.R.	7°12.0'	80°07.3'	73	
70	70-1	Y71-8-70MG3	11-12	90	8°41.9'	82°13.3'	4378	
"	70-2	Y71-8-70P	1516-1517	1521	"	"	"	
71	71-1	Y71-8-71MG1	3-4.5	97	7°35.3'	81°40.0'	5535	
"	71-2	Y71-8-71P	593-594	882	"	"	"	A. L.
72		Y71-8-72P		986	7°24.4'	81°24.8'	5846	
73	73-1	Y71-8-73P	3-4.5	206	7°23.5'	81°22.5'	5360	
74	74-1	Y71-8-74MG5	3-4.5	62	7°33.7'	81°10.3'	3968	
"	74-2	Y71-8-74P	541-542	543	"	"	"	
76	76-1	Y71-8-76MG4	5-6	88	8°07.0'	81°36.0'	5122	
77	77-1	Y71-8-77MG4	18-19	84	8°10.8'	81°35.6'	5121	
"	77-2	"	21-22	"	"	"	"	
78	78-1	Y71-8-78MG4	1-2	90	7°51.2'	81°19.5'	5760	
"	78-2	Y71-8-78P	1170-1171	1172	"	"	"	
79		Y71-8-79FF2		94	7°50.0'	81°17.0'	6165	
80		Y71-8-80FF3		73	7°48.7'	81°15.7'	6117	
81		Y71-8-81FF5		93	7°48.3'	81°15.1'	6083	
82		Y71-8-82FF6		66	7°48.0'	81°14.7'	6059	
83	83-1	Y71-8-83MG1	1-2	33	7°40.1'	81°02.6'	3103	
"	83-2	Y71-8-83P	574-575	576	"	"	"	
93	93-1	HIG 93 FFC 153	6-7.5	118	12°12.1'	83°10.4'	5158	
94	94-1	HIG 94 FFC 158	2-3.5	117	11°59.6'	81°30.0'	4646	
95	95-1	HIG 95 FFC 162	6-7.5	90	12°01.4'	79°33.9'	4904	
96	96-1	HIG 96 GC 01	6-7.5	75	12°26.8'	77°33.0'	173	
98	98-1	HIG 98 GC 07	8.5-10	123	10°30.0'	83°05.3'	~4620	

APPENDIX I. Continued

Core No.	Sample No.	Core Identification	Sample Interval (cm)	Core Length (cm)	Latitude °S	Longitude °W	Water Depth (m)
127	127-1	HIG 127 PC 71	6.5-8	453	8°38.3'	79°18.1'	~85
128	128-1	HIG 128 PC 72	2-3.5	63	7°47.9'	82°39.0'	~4240
130	130-1	HIG 130 PC 73	2-3.5	1125	7°06.8'	81°27.1'	~5240
"	130-2	HIG 130 PC 73	562-563	"	"	"	"
"	130-3	"	1121-1122	"	"	"	"
131	131-1	HIG 131 PC 74	4-5.5	343	7°05.6'	81°22.5'	~4590
"	131-2	"	172-173.5	"	"	"	"
"	131-3	"	337-338.5	"	"	"	"
132	132-1	HIG 132 PC 75	6-7.5	836	6°39.5'	81°36.8'	~4390
134	134-1	HIG 134 PC 76	1-2.5	1184	6°02.5'	83°03.9'	~4000
"	134-2	"	592-593.5	"	"	"	"
135	135-1	HIG 135 PC 77	1-2.5	452	6°00.8'	87°09.9'	~3880
R71	R71-1	RC9-71 TW	0-1	28	8°05'	83°51'	4297
R76	R76-1	RC9-76 TW	0-1	N.R.	16°37.9'	78°07.9'	3248
"	R76-2	RC9-76	~550	1100	"	"	"
"	R76-3	"	~1100	"	"	"	"
R77	R77-1	RC9-77 TW	0-1	N.R.	17°59.8'	79°09'	2880
V35	V35-1	V15-35 TW	0-1	N.R.	9°43'	80°04'	2869
"	V35-2	V15-35	~291	583	"	"	"
"	V35-3	"	~583	"	"	"	"
V43	V43-1	V15-43 TW	0-1	N.R.	8°36'	84°40.5'	4451
V545	V545-1	V15-45 TW	0-1	"	11°12'	84°48'	4459

APPENDIX I. Continued

Core No.	Sample No.	Core Identification	Sample Interval (cm)	Core Length (cm)	Latitude °S	Longitude °W	Water Depth (m)
V745	V745-1	V17-45 TW	0-1	20	7°10'	85°48'	4085
V33	V33-1	V19-33 TW	0-1	N. R.	10°40'	78°10'	177

Types of Bottom Samplers:

FF, FFC	free fall core
G	grab sample
MG	multiple gravity core
P, PC	piston core
SS	shipek grab sample
TW	trigger weight core

N. R. = Not Recorded

Special Types of Sediment:

A. L. = ash layer
D. = dolomite

APPENDIX II. Raw Data

Sample No.	% Smectite	% Mixed-Layer	% Illite	% Kaolinite	% Chlorite	% Organic Carbon
3-1	0.0	0.0	53.8	15.0	31.2	7.53
4-1	43.2	0.0	32.4	10.1	14.3	0.97
4-2	40.2	0.0	36.5	9.8	13.6	1.21
4-3	47.0	0.0	31.4	8.9	13.0	0.85
4-4	38.6	0.0	35.3	9.8	16.3	0.57
4-5	44.2	0.0	34.0	8.0	13.9	0.72
4-6	35.8	0.0	38.7	11.7	13.9	0.43
4-7	45.8	0.0	32.7	9.0	12.5	0.44
4-8	35.9	0.0	37.8	11.4	14.9	0.43
4-9	33.2	0.0	39.8	11.3	15.7	0.45
4-10	43.6	0.0	34.8	7.8	13.8	0.53
4-11	46.6	0.0	35.5	7.3	10.7	0.42
5-1	0.0	32.6	36.8	10.6	19.9	6.14
5-2	0.0	24.0	44.4	11.6	20.0	5.21
5-3	0.0	22.4	47.8	14.0	15.6	4.83
6-1	0.0	23.9	32.5	17.2	26.4	4.27
6-2	0.0	56.5	25.2	8.3	10.0	2.60
6-3	0.0	17.7	45.8	16.8	19.8	3.99
7-1	25.4	0.0	38.9	15.4	20.4	3.60
7-2	29.8	0.0	40.6	12.6	17.0	3.08
8-1	0.0	23.0	46.9	12.6	17.6	2.95
8-2	0.0	20.4	47.6	13.8	18.2	2.06
12-1	31.7	0.0	46.3	8.4	13.6	2.50
12-2	41.7	0.0	30.7	11.0	17.5	1.75
12-3	37.6	0.0	46.8	5.8	9.8	1.00
14-1	43.8	0.0	34.2	9.6	12.4	0.79
14-2	46.6	0.0	34.8	6.9	11.8	0.50
14-3	45.4	0.0	37.5	7.2	10.0	0.43
17-1	45.0	0.0	33.1	12.4	9.4	2.39
17-2	39.8	0.0	34.2	13.8	12.0	1.35
19-1	39.8	0.0	38.2	9.4	12.6	0.72
19-2	40.0	0.0	44.4	6.3	9.4	0.62
21-1	51.7	0.0	30.4	10.8	7.2	2.35
21-2	47.4	0.0	33.8	10.4	8.4	2.10
22-1	46.3	0.0	32.4	11.8	9.6	3.49
22-2	36.8	0.0	40.0	12.0	11.0	4.07
22-3	39.0	0.0	34.1	12.8	13.9	3.57
23-1	0.0	40.8	26.4	14.8	18.0	4.15
24-1	40.5	0.0	38.8	8.2	12.5	1.69

APPENDIX II. Continued

Sample No.	% Smectite	% Mixed-Layer	% Illite	% Kaolinite	% Chlorite	% Organic Carbon
24-2	0.0	43.4	32.0	9.1	15.6	4.19
24-3	41.8	0.0	37.3	8.0	12.9	1.24
24-4	43.9	0.0	37.9	7.2	11.3	1.39
24-5	41.5	0.0	40.2	7.0	11.2	2.14
24-6	0.0	37.8	25.6	11.4	25.2	5.13
25-1	0.0	43.8	29.6	9.4	17.2	2.74
25-2	36.0	0.0	42.6	9.2	12.2	1.46
27-1	39.9	0.0	39.6	10.2	10.3	0.59
28-1	38.2	0.0	40.4	11.0	10.4	1.39
55-1	33.0	0.0	39.2	11.2	16.7	1.58
55-2	0.0	15.0	46.6	13.6	24.6	4.43
56-1	30.9	0.0	44.2	12.0	13.0	1.65
56-2	0.0	13.6	46.4	15.0	24.8	5.19
57-1	32.0	0.0	46.0	8.6	13.5	2.37
57-2	0.0	22.1	48.4	10.1	19.4	2.50
58-1	24.6	0.0	46.4	13.8	15.2	1.63
58-2	0.0	20.4	40.0	18.3	21.4	4.14
59-1	40.9	0.0	38.2	10.0	10.8	1.41
59-2	17.4	0.0	50.6	13.4	18.6	1.51
61-1	29.5	0.0	44.8	13.3	12.4	1.75
61-2	17.1	0.0	50.6	13.2	18.6	2.76
65-1	41.3	0.0	38.4	9.1	11.3	1.53
65-2	20.9	0.0	47.7	14.6	16.6	2.07
68-1	0.0	10.0	45.6	16.6	27.8	1.25
70-1	42.0	0.0	33.0	10.8	14.3	1.23
70-2	33.6	0.0	40.4	10.5	15.4	1.19
71-1	36.6	0.0	44.0	9.9	9.5	1.56
73-1	0.0	19.4	43.3	16.3	21.0	2.19
74-1	24.0	0.0	44.3	16.6	15.0	2.65
74-2	0.0	11.2	53.2	14.6	21.2	2.25
76-1	23.0	0.0	43.4	15.1	18.5	2.39
77-1	0.0	30.1	45.0	11.2	13.7	3.03
77-2	35.6	0.0	46.1	9.4	8.8	1.51
78-1	32.5	0.0	40.9	13.6	13.0	1.97
78-2	12.7	0.0	52.2	14.5	20.6	1.77
83-1	30.8	0.0	42.2	14.3	12.6	3.73
83-2	29.2	0.0	41.5	14.2	15.1	2.90
93-1	37.2	0.0	45.3	8.2	9.4	0.56
94-1	40.2	0.0	42.2	7.6	10.0	0.66

APPENDIX II. Continued

Sample No.	% Smectite	% Mixed-Layer	% Illite	% Kaolinite	% Chlorite	% Organic Carbon
95-1	37.4	0.0	43.9	7.8	10.8	1.00
96-1	0.0	11.6	47.8	17.8	22.8	7.52
98-1	40.6	0.0	44.2	7.0	8.4	0.67
127-1	14.6	0.0	56.8	9.5	19.1	0.96
128-1	33.0	0.0	43.2	11.2	12.7	1.78
130-1	36.0	0.0	44.4	11.2	8.4	3.75
130-2	38.0	0.0	44.0	9.8	8.2	2.99
130-3	36.4	0.0	42.4	9.8	11.4	2.35
131-1	34.9	0.0	42.8	11.4	11.0	3.26
131-2	27.6	0.0	47.9	9.3	15.3	2.30
131-3	23.2	0.0	49.0	9.8	18.0	2.14
132-1	36.2	0.0	36.1	12.3	15.4	2.03
134-1	54.0	0.0	26.6	7.4	12.0	2.50
134-2	47.2	0.0	32.8	8.9	11.0	1.99
135-1	100.0	0.0	0.0	0.0	0.0	2.24
R71-1	43.6	0.0	34.0	11.2	11.1	1.72
R76-1	47.2	0.0	34.1	7.0	11.6	2.07
R76-2	60.6	0.0	26.5	5.2	7.6	1.43
R76-3	53.0	0.0	30.6	7.4	9.0	1.65
R77-1	50.6	0.0	26.0	10.6	12.6	0.88
V35-1	26.8	0.0	48.8	12.2	12.2	3.21
V35-2	0.0	20.3	51.7	9.6	18.4	4.87
V35-3	0.0	17.0	56.0	8.2	18.8	4.18
V43-1	38.1	0.0	47.0	7.7	7.2	1.70
V545-1	41.8	0.0	41.3	8.0	9.0	1.09
V745-1	44.2	0.0	37.8	9.2	8.8	2.10
V33-1	0.0	0.0	61.6	12.2	26.3	5.96

APPENDIX III. Varimax Factor Matrix

Sample No.	Communality	Factor 1 Oceanic	Factor 2 Contl A	Factor 3 Contl B
3-1	.975	.370	.670	-0.624
4-1	.993	.944	.282	-0.148
4-2	.998	.921	.322	-0.212
4-3	.979	.955	.236	-0.104
4-4	.972	.901	.338	-0.216
4-5	.978	.939	.272	-0.152
4-6	.980	.878	.369	-0.270
4-7	.981	.950	.249	-0.125
4-8	.978	.879	.368	-0.262
4-9	.979	.851	.402	-0.305
4-10	.979	.935	.280	-0.164
4-11	.982	.950	.245	-0.142
5-1	.993	.246	.959	-0.111
5-2	.975	.305	.891	-0.297
5-3	.965	.324	.863	-0.341
6-1	.974	.262	.930	-0.198
6-2	.943	.095	.921	.291
6-3	.977	.333	.844	-0.392
7-1	.978	.766	.498	-0.378
7-2	.977	.814	.443	-0.344
8-1	.988	.321	.881	-0.331
8-2	.975	.329	.855	-0.369
12-1	.996	.827	.422	-0.366
12-2	.960	.921	.300	-0.147
12-3	.970	.868	.350	-0.307
14-1	.998	.947	.276	-0.157
14-2	.980	.949	.246	-0.136
14-3	.981	.941	.260	-0.168
17-1	.996	.956	.255	-0.134
17-2	.974	.916	.314	-0.191
19-1	.999	.917	.326	-0.229
19-2	.974	.893	.324	-0.269
21-1	.998	.982	.178	-0.053
21-2	.982	.957	.229	-0.118
22-1	.996	.961	.242	-0.116
22-2	.979	.883	.357	-0.268
22-3	.974	.909	.329	-0.200
23-1	.998	.165	.979	.112
24-1	.998	.919	.321	-0.227
24-2	.963	.178	.961	.083

APPENDIX III. Continued

Sample No.	Communality	Factor 1 Oceanic	Factor 2 Contl A	Factor 3 Contl B
24-3	.981	.922	.303	-0.201
24-4	.982	.932	.280	-0.186
24-5	.980	.913	.308	-0.226
24-6	.967	.166	.967	.073
25-1	.987	.165	.973	.113
25-2	.983	.871	.369	-0.296
27-1	.999	.916	.322	-0.237
28-1	.999	.902	.343	-0.260
55-1	.995	.856	.410	-0.306
55-2	.980	.337	.824	-0.433
56-1	.999	.829	.428	-0.360
56-2	.979	.340	.813	-0.449
57-1	.996	.831	.419	-0.361
57-2	.969	.322	.861	-0.351
58-1	.999	.752	.494	-0.434
58-2	.973	.307	.884	-0.313
59-1	1.000	.925	.311	-0.217
59-2	.984	.641	.555	-0.515
61-1	.997	.813	.441	-0.376
61-2	.983	.637	.557	-0.517
65-1	1.000	.926	.310	-0.215
65-2	.981	.695	.525	-0.471
68-1	.981	.347	.787	-0.492
70-1	.993	.938	.295	-0.162
70-2	.980	.854	.398	-0.305
71-1	.994	.880	.361	-0.301
73-1	.998	.324	.875	-0.357
74-1	.993	.749	.500	-0.426
74-2	.983	.363	.766	-0.514
76-1	.993	.734	.518	-0.432
77-1	.947	.286	.905	-0.214
77-2	.973	.858	.368	-0.321
78-1	.998	.853	.409	-0.321
78-2	.983	.571	.590	-0.555
83-1	.996	.832	.428	-0.346
83-2	.977	.808	.446	-0.355
93-1	.990	.879	.355	-0.304
94-1	.994	.909	.323	-0.254
95-1	.994	.884	.355	-0.293
96-1	.992	.353	.796	-0.484

APPENDIX III. Continued

Sample No.	Communality	Factor 1 Oceanic	Factor 2 Contl A	Factor 3 Contl B
98-1	.989	.904	.318	-0.263
127-1	.991	.595	.568	-0.561
128-1	.999	.851	.406	-0.332
130-1	.991	.873	.367	-0.307
130-2	.976	.882	.343	-0.284
130-3	.981	.874	.364	-0.290
131-1	.998	.869	.383	-0.310
131-2	.980	.773	.462	-0.411
131-3	.980	.717	.506	-0.458
132-1	.993	.892	.369	-0.248
134-1	.992	.984	.155	-0.005
134-2	.983	.957	.234	-0.113
135-1	.993	.912	-0.190	.354
R71-1	.998	.948	.275	-0.156
R76-1	.997	.961	.241	-0.126
R76-2	.985	.987	.089	.042
R76-3	.982	.976	.169	-0.046
R77-1	.988	.977	.183	-0.024
V35-1	.995	.772	.467	-0.425
V35-2	.959	.333	.833	-0.392
V35-3	.958	.349	.793	-0.455
V43-1	.982	.879	.343	-0.304
V545-1	.995	.921	.304	-0.232
V745-1	.999	.944	.274	-0.182
V33-1	.995	.385	.650	-0.651